Characterization and analysis of edges in piecewise smooth functions

Kanghui Guo

Department of Mathematics, Missouri State University, Springfield, Missouri 65804, USA

Demetrio Labate

Department of Mathematics, University of Houston, 651 Phillip G Hoffman, Houston, TX 77204-3008, USA

Abstract

The analysis and detection of edges is a central problem in applied mathematics and image processing.

A number of results in recent years have shown that directional multiscale methods such as continuous curvelet and shearlet transforms offer a powerful theoretical framework to capture the geometry of edge singularities, going far beyond the capabilities of the conventional wavelet transform. The continuous shearlet transform, in particular, provides a precise geometric characterization of edges in piecewise constant functions in $\mathbb{R}^2$ and $\mathbb{R}^3$, including corner points. However, a question has been raised frequently: What happens if the function is piecewise smooth and not just piecewise constant? Clearly, a piecewise smooth function is a much more realistic model of images with edges.

In this paper, we extend the characterization results previously known and show that, also in the case of piecewise smooth functions, the continuous shearlet transform can detect the location and orientation of edge points, including corner points, through its asymptotic decay at fine scales. The new proof introduces some innovative technical constructions to deal with the more challenging problem. The new results set the theoretical groundwork for the application of the shearlet framework to a wider class of problems from image processing.

Keywords: Analysis of singularities; continuous wavelets; curvelets; directional wavelets; edge detection; shearlets; wavelets.

1. Introduction

Multiscale methods and wavelets have been frequently associated with the analysis of singularities of functions and distributions and the application of

Email addresses: KanghuiGuo@MissouriState.edu (Kanghui Guo), dlabate@math.uh.edu (Demetrio Labate)

the wavelet transform to edge detection goes back to the origins of the wavelet literature [10]. In fact, it is not difficult to show that, if f is a function that is smooth apart from a discontinuity at a point p_0, then the continuous wavelet transform of f, denoted by $\mathcal{W}f(a,p)$, decays rapidly at asymptotically finer scales (as a approaches 0) unless p is near p_0 [17, 28]. More generally, one can show that the continuous wavelet transform resolves the *singular support* of f, that is, the set of points where f is not regular, and can be applied to measure the pointwise regularity of functions [18, 19].

However, the conventional wavelet approach is unable to provide additional information about the *geometry* of the set of singularities of f. In many applications, including propagation of singularities in PDEs and image processing, it is useful not only to identify the locations of the singular points, but also their geometrical properties, such as the orientation and curvature of an edge.

In the mathematical literature, the idea of using generalized wavelet-like transforms to perform a more sophisticated microlocal analysis of singularities can be traced back to Bros and Iagolnitzer [1] and Cordoba and Fefferman [3], who both defined transforms with implicitly a kind of anisotropic scaling. It was later shown that the Fourier-Bros-Iagolnitzer (FBI) transform is able to resolve not only the singular support but also the wavefront set of a distribution [8]. During the last decade, following the introduction of a new generation of directional multiscale systems in the wavelet literature, most notably the curvelet [2] and shearlet systems [21], it was shown that it is possible to define "generalized" wavelet transforms able to resolve the wavefront set of distributions [9, 21]. Among such transforms, the continuous shearlet transform offers an especially appealing mathematical framework, due to a simple construction, derived from the general setting of affine systems, and its high directional sensitivity obtained through the action of anisotropic dilations and shear transformations. One major advantage of this approach is that, thanks to the affine structure, there is a rather direct procedure to derive discrete versions of the shearlet transform and transfer the theoretical properties of the continuous transform to its discrete counterparts [7, 23].

In particular, it was shown by the authors and their collaborators that the continuous shearlet transform provides a precise *geometric* characterization of edge singularities for a large class of multidimensional functions and distributions [12, 13, 14, 15], going far beyond the capabilities of wavelets and other conventional multiscale methods. For example, let us consider piecewise constant functions of the form $h = \sum_{i=1}^{N} c_i \chi_{S_i}$, where, for each i, c_i is a constant and S_i is a compact subset of $\mathbb{R}^2$. Such functions provide a very simple model of images with edges where the edge detection problem consists in identifying the boundary curves ∂S_i of the sets S_i. The continuous shearlet transform was found to be remarkably effective for this task, since it precisely characterizes the *location* and *orientation* of piecewise regular boundary curves ∂S_i, including possibly corner points[1]. Similar results were found in the three-dimensional

[1]Note that corner points and junctions frequently provide the most conspicuous and useful

setting [13, 14]. We also mention a very recent version of these results using compactly supported shearlet generators by Kutyniok and Petersen [22], which includes uniform estimates.

The theoretical results available so far, however, are restricted for the most part to a very simplified model of images consisting of piecewise constant functions (cf. [11] for a recent survey about these theoretical results). To go beyond this limitation, in this paper, we consider a much more realistic model of images with edges that is not limited to characteristic functions of sets, but includes general smooth density functions. The geometric analysis and detection of edges in this situation is significantly more challenging and cannot be handled using the techniques and arguments developed in the previous studies. In order to illustrate these challenges and describe the main original contributions of this work, let us start by setting our notation and recalling the results currently known (in dimensions $n = 2$).

In this paper, we consider functions of the form

$$h(x) = \sum_{i=1}^{N} f_i(x)\, \chi_{S_i}(x), \tag{1.1}$$

where, for each i, f_i is a C^∞ (non-trivial) function and S_i is a compact region in $\mathbb{R}^2$ whose boundary, denoted by ∂S_i, is a simple, *piecewise smooth* curve, of finite length. To simplify our arguments, we assume that the regions S_i are mutually disconnected, that is, they do not overlap and share no boundary curves. At the end of this paper, in Sec. 6, we will outline the steps on how to extend our arguments to the more general case where the sum in (1.1) includes regions S_i sharing common boundary curves.

Under the assumption that the regions S_i are mutually disconnected, the finite sum over i in (1.1) does not play any role in our analysis. This is due to the fact that the shearlet-based analysis is highly local (cf. Lemma 4.2), that is, shearlet decay estimates at an edge point p only depends on the behavior of the function in a small neighborhood of p. Therefore, in the following, we will ignore the sum and simply consider functions of the form $B = f\, \chi_S$.

Let $\vec{\alpha}(t)$ be the parametrization of ∂S with respect to the arc length parameter t. For any $t_0 \in (0, L)$ and any $j \geq 0$, we denote by $\vec{\alpha}^{(j)}(t)$ the j-th derivative of $\vec{\alpha}(t)$, and assume that $\lim_{t \to t_0^-} \vec{\alpha}^{(j)}(t) = \vec{\alpha}^{(j)}(t_0^-)$ and $\lim_{t \to t_0^+} \vec{\alpha}^{(j)}(t) = \vec{\alpha}^{(j)}(t_0^+)$ exist. Also, let $\vec{n}(t^-)$, $\vec{n}(t^+)$ be the outer normal direction(s) of ∂S at $\vec{\alpha}(t)$ from the left and right, respectively. We say that $p = \vec{\alpha}(t_0)$ is a *corner point of* ∂S if $\vec{\alpha}'(t_0^-) \neq \pm\vec{\alpha}'(t_0^+)$ On the other hand, if $\vec{\alpha}(t)$ is infinitely many times differentiable at t_0, we say that $\vec{\alpha}(t_0)$ is a *regular point* of ∂S. Finally, we say that the boundary curve $\vec{\alpha}(t)$ is *piecewise smooth* if $\vec{\alpha}(t)$ are regular points for all $0 \leq t \leq L$, except for finitely many corner points.

To detect the discontinuities of the function B, we will apply the continuous

features for many algorithms of edge analysis and feature extraction (e.g. [25, 33]).

shearlet transform defined as a mapping

$$\mathcal{SH}_\psi : B \longrightarrow \mathcal{SH}_\psi B(a,s,p), \quad a>0, s\in\mathbb{R}, p\in\mathbb{R}^2,$$

where the variables (a, s, p) are associated with notions of scale, orientation and location, respectively. The precise definition of $\mathcal{SH}_\psi$ will be given in Section 2.

In the special case where f is a constant function, the shearlet-based geometric characterization of the set of discontinuities of f is well known. Let $p = \vec{\alpha}(t_0)$ be a regular point of ∂S and $s = \tan(\theta_0)$ with $\theta_0 \in (-\frac{\pi}{2}, \frac{\pi}{2})$. Let $\Theta(\theta_0) = (\cos\theta_0, \sin\theta_0)$. We say that *s corresponds to the normal direction* of ∂S at p if $\Theta(\theta_0) = \pm\vec{n}(t_0)$. The following theorem from [12] (that extends and refines partial results previously obtained in [2, 15, 21]) shows that $\mathcal{SH}_\psi B(a, s, p)$ has rapid asymptotic decay when $a \to 0$ for all values of s, p, unless $p \in \partial S$ and s corresponds to the normal direction of ∂S at p.

Theorem 1.1. *Let $B = \chi_S$, where S is a compact subset of $\mathbb{R}^2$ with piecewise smooth boundary ∂S.*

(i) If $p \notin \partial S$ then

$$\lim_{a\to 0^+} a^{-N}\, \mathcal{SH}_\psi B(a, s_0, p) = 0, \qquad \textit{for all } N > 0.$$

(ii) If $p \in \partial S$ is a regular point and $s = s_0$ does not correspond to the normal direction of ∂S at p then

$$\lim_{a\to 0^+} a^{-N}\, \mathcal{SH}_\psi B(a, s_0, p) = 0, \qquad \textit{for all } N > 0.$$

(iii) If $p \in \partial S$ is a regular point and $s = s_0$ corresponds to the normal direction of ∂S at p then

$$\lim_{a\to 0^+} a^{-\frac{3}{4}}\, \mathcal{SH}_\psi B(a, s_0, p) \neq 0.$$

The next result, also from [12], shows that a similar behavior is observed when $p = \vec{\alpha}(t_0)$ is a corner point. In this case, however, there are two outer normal directions $\vec{n}(t_0^-)$ and $\vec{n}(t_0^+)$.

Theorem 1.2. *Let B and S be as in Theorem 1.1.*

(i) If $p \in \partial S$ is a corner point and $s = s_0$ does not correspond to any of the normal directions of ∂S at p, then

$$\lim_{a\to 0^+} a^{-\frac{9}{4}}\, |\mathcal{SH}_\psi B(a, s_0, p)| < \infty.$$

(ii) If $p \in \partial S$ is a corner point and $s = s_0$ corresponds to one of the normal directions of ∂S at p then

$$0 < \lim_{a\to 0^+} a^{-\frac{3}{4}}\, |\mathcal{SH}_\psi B(a, s_0, p)| < \infty.$$

The most difficult and critical part in the proof of the above results is the 'lower bound estimate' (part (iii) of Theorem 1.1 and part (ii) of Theorem 1.2), because it involves the existence of a non-vanishing limit point. The original argument in [12] relies on the quadratic approximation of the boundary curve ∂S and the method of stationary phase, so that the ∂S can be locally approximated with the arc of a circle; then one can use the special-case result of the shearlet transform of the indicator function of the disc, that was studied by the authors in [15]. This approach fails when $B = f\chi_S$, due to the presence of the smooth density function f that may possibly vanish on ∂S together with multiple derivatives.

In this paper, to deal with the function $B = f\chi_S$ we introduce a new approach that does not use the local approximation of the boundary ∂S nor the method of stationary phase. However, the new proof requires the use of two different generator functions for the analyzing shearlet system, designed to deal with boundary points having curvatures near zero and away from zero respectively. Apart from this additional technical requirement, the new theorems we obtain are stated very similarly to the theorems above. That is, also for this more general class of functions, the continuous shearlet transform of $B = f\chi_S$ provides a precise geometric characterization of the discontinuity curve ∂B through it asymptotic decay at fine scales. The precise statement of this results will be given in Section 3.

The rest of the paper is organized as follows. In Section 2, we recall the definition and main properties of the continuous shearlet transform. In Section 3, we present our new main theorems and describe the organization of the proof. In Section 4, we derive a variant of the Divergence theorem and develop some localization lemmata. In Section 5, we present the proofs of the new theorems.

2. The shearlet transform

In this section, we recall the definition and basic properties of the continuous shearlet transform (cf. [4, 21]).

Let $\psi^{(\mathfrak{h})}, \psi^{(\mathfrak{v})} \in L^2(\mathbb{R}^2)$ and, for $a > 0$ and $s \in \mathbb{R}$, let

$$M_{as} = \begin{pmatrix} a & -a^{1/2}s \\ 0 & a^{1/2} \end{pmatrix}, \quad N_{as} = \begin{pmatrix} a^{1/2} & 0 \\ -a^{1/2}s & a \end{pmatrix}.$$

We define the *horizontal* and *vertical (continuous) shearlets* generated by $\psi^{(\mathfrak{h})}, \psi^{(\mathfrak{v})}$ as the collections of functions

$$\psi^{(\mathfrak{h})}_{asp}(x) = |\det M_{as}|^{-\frac{1}{2}} \psi^{(\mathfrak{h})}(M_{as}^{-1}(x-p)), \quad a > 0, s \in \mathbb{R}, p \in \mathbb{R}^2,$$

and

$$\psi^{(\mathfrak{v})}_{asp}(x) = |\det N_{as}|^{-\frac{1}{2}} \psi^{(\mathfrak{v})}(N_{as}^{-1}(x-p)), \quad a > 0, s \in \mathbb{R}, p \in \mathbb{R}^2,$$

respectively. The reason for the wording 'horizontal' and 'vertical' will become clear below.

Under appropriate *admissibility conditions* on of the generators $\psi^{(\mathfrak{h})}, \psi^{(\mathfrak{v})}$, the continuous shearlets $\{\psi_{asp}^{(\mathfrak{h})}\}$ and $\{\psi_{asp}^{(\mathfrak{v})}\}$ form reproducing systems for certain subspaces of $L^2(\mathbb{R}^2)$. Specifically, let us consider the following horizontal or vertical cone-shaped regions in the Fourier domain:

$$\begin{aligned}
\mathcal{P}^{(\mathfrak{h})} &= \{(\xi_1,\xi_2) \in \mathbb{R}^2 : |\xi_1| \geq 2 \text{ and } |\tfrac{\xi_2}{\xi_1}| \leq 1\}, \\
\mathcal{P}^{(\mathfrak{v})} &= \{(\xi_1,\xi_2) \in \mathbb{R}^2 : |\xi_1| \geq 2 \text{ and } |\tfrac{\xi_2}{\xi_1}| > 1\};
\end{aligned}$$

and let

$$L^2(\mathcal{P}^{(\mathfrak{h})})^\vee = \{f \in L^2(\mathbb{R}^2) : \operatorname{supp} \hat{f} \subset \mathcal{P}^{(\mathfrak{h})}\},$$

with a similar definition for $L^2(\mathcal{P}^{(\mathfrak{v})})^\vee$. The following proposition, which is a generalization of a result in [21], shows that the horizontal and vertical shearlets form a continuous reproducing system for the spaces $L^2(\mathcal{P}^{(\mathfrak{h})})^\vee$ and $L^2(\mathcal{P}^{(\mathfrak{v})})^\vee$, respectively.

Proposition 2.1. *For $\xi = (\xi_1, \xi_2) \in \mathbb{R}^2$, let $\psi^{(\mathfrak{h})}$ and $\psi^{(\mathfrak{v})}$ be given by*

$$\hat{\psi}^{(\mathfrak{h})}(\xi_1,\xi_2) = w(\xi_1)\, v(\tfrac{\xi_2}{\xi_1}), \quad \hat{\psi}^{(\mathfrak{v})}(\xi_1,\xi_2) = w(\xi_2)\, v(\tfrac{\xi_1}{\xi_2}), \tag{2.1}$$

where w, v satisfy the conditions:

$$\int_0^\infty |w(a\omega)|^2 \frac{da}{a} = 1, \text{ for a.e. } \omega \in \mathbb{R}; \operatorname{supp} w \subset [-2,-\tfrac{1}{2}] \cup [\tfrac{1}{2},2]; \tag{2.2}$$

$$\|v\|_2 = 1 \quad \text{and} \quad \operatorname{supp} v \subset [-1,1]. \tag{2.3}$$

We then have that, for all $f \in L^2(\mathcal{P}^{(d)})^\vee$,

$$f = \int_{\mathbb{R}^2} \int_{-2}^{2} \int_0^{\frac{1}{4}} \langle f, \psi_{asp}^{(d)} \rangle\, \psi_{asp}^{(d)} \frac{da}{a^3}\, ds\, dp,$$

where $d = \mathfrak{h}$ or $d = \mathfrak{v}$ and the equality is understood in the L^2 sense.

Note that $\frac{da}{a^3}\, ds\, dp$ is the left Haar measure of the so-called shearlet group (cf. [4, 5]).

There are several examples of admissible shearlet generators of the form (2.1) satisfying conditions (2.2) and (2.3), including function that are C^∞ and compactly supported in the Fourier domain [15, 21]. A simple computation shows that, in the Fourier domain, a representative horizontal shearlet $\psi_{asp}^{(\mathfrak{h})}$ has the form:

$$\hat{\psi}_{asp}^{(\mathfrak{h})}(\xi_1,\xi_2) = a^{\frac{3}{4}}\, w(a\,\xi_1)\, v(a^{-1/2}(\tfrac{\xi_2}{\xi_1} - s))\, e^{-2\pi i \xi \cdot p}.$$

This implies that the function $\hat{\psi}_{asp}^{(\mathfrak{h})}$ has support:

$$\operatorname{supp} \hat{\psi}_{asp}^{(\mathfrak{h})} \subset \{(\xi_1,\xi_2) : \xi_1 \in [-\tfrac{2}{a}, -\tfrac{1}{2a}] \cup [\tfrac{1}{2a}, \tfrac{2}{a}],\ |\tfrac{\xi_2}{\xi_1} - s| \leq a^{1/2}\}.$$

That is, the support of $\hat{\psi}_{asp}^{(\mathfrak{h})}$ is contained inside a pair of trapezoidal regions, symmetric with respect to the origin, oriented along a line of slope s. The

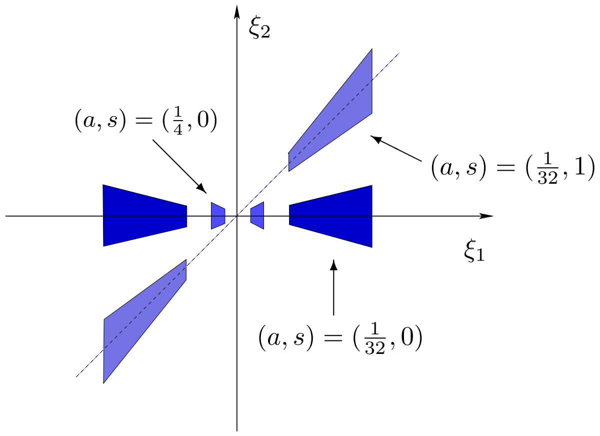

Figure 1: Supports of representative shearlets $\hat{\psi}^{(\mathfrak{h})}_{asp}$ (in the Fourier domain) for different values of a and s.

support becomes increasingly elongated as $a \to 0$. This is illustrated in Fig. 1. The shearlets $\psi^{(\mathfrak{v})}_{asp}$ have similar properties, with frequency supports oriented along lines of slopes $\frac{1}{s}$.

We define the *(fine-scale) continuous shearlet transform* on $L^2(\mathbb{R}^2)$ as the mapping

$$f \in L^2(\mathbb{R}^2 \setminus [-2,2]^2)^\vee \to \mathcal{SH}_\psi f(a,s,p), \quad a \in (0, \tfrac{1}{4}], s \in [-\infty, \infty], p \in \mathbb{R}^2,$$

given by

$$\mathcal{SH}_\psi f(a,s,p) = \begin{cases} \mathcal{SH}^{(\mathfrak{h})}_\psi f(a,s,p) = \langle f, \psi^{(\mathfrak{h})}_{a,s,p} \rangle, & \text{if } |s| \le 1 \\ \mathcal{SH}^{(\mathfrak{v})}_\psi f(a, \frac{1}{s}, p) = \langle f, \psi^{(\mathfrak{v})}_{a,s,p} \rangle, & \text{if } |s| > 1. \end{cases} \tag{2.4}$$

In this expression, it is understood that the limit values $s = \pm\infty$ are defined and that we have $\mathcal{SH}_\psi f(a, \pm\infty, p) = \mathcal{SH}^{(\mathfrak{v})}_\psi f(a, 0, p)$.

The continuous shearlet transform maps a function f into a continuous collection of coefficients $\mathcal{SH}_\psi f(a,s,p)$ depending on the *scale* $a \in (0, 1/4]$, the *orientation* $s \in \mathbb{R}$ and the *location* $p \in \mathbb{R}^2$. The term *fine-scale* refers to the fact that this shearlet transform is only defined for $a \in (0, 1/4]$ (rather than $a > 0$), corresponding to "fine scales". In fact, as it is clear from Proposition 2.1, the shearlet transform $\mathcal{SH}_\psi f$ defines an isometry on $L^2(\mathbb{R}^2 \setminus [-2,2]^2)^\vee$, the subspace of $L^2(\mathbb{R}^2)$ of functions with frequency support away from $[-2,2]^2$, but not on $L^2(\mathbb{R}^2)$. This is not a limitation since our geometric characterization of singularities will derive asymptotic estimates as a approaches 0.

We remark that, for the application of the continuous shearlet transform to the study of singularities, some special care must be taken in the choice of the shearlet generator. We recall that the proofs of Theorems 1.1 and 1.2 in [12] require that the shearlet generators satisfy conditions (2.1), (2.2), (2.3), that w

is a C^∞ odd function, non-negative on the positive axis, and that v is a C^∞ even function. In this paper, since we use a very different argument for the 'lower bound' estimate, we need different assumptions. We will still consider a generator of the form (2.1) where, however, we will now require:

- $w \in C_c^\infty(\mathbb{R}),\ \operatorname{supp} w \subset [-1,1],$ is odd, nonnegative on $[0,1]$ and it satisfies $\displaystyle\int_0^\infty |w(a\xi)|^2 \,\frac{da}{a} = c_1 \neq 0;$
- $v \in C_c^\infty(\mathbb{R}),\ \operatorname{supp} v \subset [-1,1],$ nonnegative and $\|v\|_2 = c_2 \neq 0.$

In particular, we can choose

$$w(\xi_1) = \begin{cases} e^{-(\frac{1}{\xi_1}+\frac{1}{1-\xi_1})}, & \text{if } \xi_1 \in (0,1) \\ 0 & \text{if } \xi_1 = 0 \\ -e^{-(\frac{1}{-\xi_1}+\frac{1}{1+\xi_1})}, & \text{if } \xi_1 \in (-1,0) \end{cases} \tag{2.5}$$

or also $w_M(\xi_1) = w(M^2\xi_1)$, for some $M \neq 0$. Note that $w \in C_c^\infty([-1,1])$ and is nonnegative on $[0,1]$. For v we can choose

$$v(\xi_2) = e^{\xi_2 - \frac{1}{1-|\xi_2|^2}}. \tag{2.6}$$

Note that $v \in C_c^\infty([-1,1])$ and is nonnegative on $[-1,1]$. We also have $v^{(n)}(0) = e^{-1}$ for all $n \geq 0$ and this property will be useful in the proof of our main theorems.

With these choices of w, w_M and v, we can define the horizontal shearlet generators $\psi^{(\mathfrak{h})}, \psi_M^{(\mathfrak{h})}$ by

$$\hat\psi^{(\mathfrak{h})}(\xi_1,\xi_2) = w(\xi_1)\, v(\tfrac{\xi_2}{\xi_1}) \quad \text{and} \quad \hat\psi_M^{(\mathfrak{h})}(\xi_1,\xi_2) = w_M(\xi_1)\, v(\tfrac{\xi_2}{\xi_1}), \tag{2.7}$$

with a similar definition for the vertical shearlet generators $\psi^{(\mathfrak{v})}, \psi_M^{(\mathfrak{v})}$. For the study of singularities that will be presented in the next section, we will need the combined action of two shearlet transforms $\mathcal{SH}_\psi$ and $\mathcal{SH}_{\psi_M}$ associated with two types of shearlet generators.

3. Main results

Let $B = f\chi_S$ where, as in stated in Section 1, $f \in C^\infty(\mathbb{R}^2)$ and $S \subset \mathbb{R}^2$ is a compact region with piecewise smooth boundary ∂S. To carry out our analysis, it will be convenient to introduce a parametrization for the curve ∂S. We will consider separately the cases where $p = (p_1, p_2) \in \partial S$ is a regular point or a corner point.

If $p \in \partial S$ is a regular point, near p we may parametrize ∂S as $\{(G(u), u), u \in U\}$, where U is a small neighborhood of p_2 and G is a smooth function, or as $\{(u, G(u)), u \in \widetilde{U}\}$, where $\widetilde{U}$ is a small neighborhood of p_1. As we will argue below, for our arguments it will be sufficient to consider only one of the two parametrizations.

To clarify this point, let us denote the horizontal shearlet system by $\Psi_{\mathfrak{h}}$ and the vertical shearlet system by $\Psi_{\mathfrak{v}}$. Also, let us denote the first type of parametrized curve by C_1 and the second one by C_2. Our arguments will consist in examining the asymptotic decay properties of the continuous shearlet transform (2.4), for $a \to 0$, near $p \in \partial S$. It turns out that, when the pair $(\Psi_{\mathfrak{h}}, C_1)$ gives a slow asymptotic decay (as the shear variable s corresponds to a normal direction near the x-axis), then the pair $(\Psi_{\mathfrak{h}}, C_2)$ will automatically produce a fast asymptotic decay (since the shear variable s will *not* correspond to the normal direction for C_2). Similarly, when the pair $(\Psi_{\mathfrak{v}}, C_2)$ gives a slow asymptotic decay (as the shear parameter s corresponds to a normal direction near the y-axis) then the pair $(\Psi_{\mathfrak{v}}, C_1)$ produce a fast asymptotic decay (since the shear variable s will *not* correspond to the normal direction for C_1). Thus, it is enough to consider either the pair $(\Psi_{\mathfrak{h}}, C_1)$ or the pair $(\Psi_{\mathfrak{v}}, C_2)$ as they produce a slow asymptotic decay as compared to the other two pairs $(\Psi_{\mathfrak{h}}, C_2)$, $(\Psi_{\mathfrak{v}}, C_1)$ which give fast asymptotic decay. Since the analysis of two cases is very similar, in the following we only consider the pair $(\Psi_{\mathfrak{h}}, C_1)$.

If $p \in \partial S$ is a corner point, we can write the curve near p as the union of two sections of curves meeting at p. For the same reason explained above, it is sufficient to consider either the horizontal shearlet system $\Psi_{\mathfrak{h}}$ with both left and right sections of curve near p parametrized as C_1 curves or the vertical shearlet system $\Psi_{\mathfrak{v}}$ with both left and right sections of curve near p parametrized as C_2 curves. As the two cases are very similar, we will only consider the first situation.

Hence, near a corner point p, we will write $\partial S = \{(G_1(u), u), u \in U_1\} \bigcup \{(G_2(u), u), u \in U_2\}$, where, for some small $\epsilon > 0$, $U_1 = [u_p, u_p + \epsilon)$, $U_2 = (u_p - \epsilon, u_p]$ and $p = (G_1(u_p), u_p) = (G_2(u_p), u_p)$. Here G_1 is smooth on U_1 and G_2 is smooth on U_2. In this case, we use the notation $f_G(u) = f(G(u), u)$, and $f_{G_1}(u) = f(G_1(u), u)$, $f_{G_2}(u) = f(G_2(u), u)$.

We make a minor technical assumption on f_G. We assume that there exists a number $N_0 \in \mathbb{N}$ such that, for any regular point $p = (G(u_p), u_p) \in \partial S$, $f_G^{(n)}(u_p) \neq 0$ for some $n \leq N_0$. Similarly, for any corner point p, we assume that, for some $0 \leq n_1,\ n_2 \leq N_0$, we have $f_{G_1}^{(n_1)}(u_p^+) \neq 0$, $f_{G_2}^{(n_2)}(u_p^-) \neq 0$. This is a very mild requirement. Since ∂S is compact, the above assumption is equivalent to say, there is no $p \in \partial S$ for which $f_G,\ f_{G_1},\ f_{G_2}$ and all its derivatives (or one-sided derivatives) are equal to zero at u_p.

Corresponding to N_0, we now want to fix the constant M that appears in the definition of the shearlet generator (2.7) and that we will need to state our main theorems. We first set the constant M_1 by

$$M_1 = 2e\,(2\pi)^{N_0} \left(\int_0^1 w(\rho)\,\tfrac{d\rho}{\rho} \right)^{-1} \int_0^1 w(\rho)\,\tfrac{d\rho}{\rho^{N_0+2}} \max_{0 \leq n \leq N_0} \int_{\mathbb{R}} |\check{v}(u)||u|^{n+2} du, \tag{3.1}$$

where w is given by (2.5) and $\check{v}$ is the inverse Fourier transform of v, given by (2.6). Next, we need the following identities for $(e^{g(t)})^{(n)}$, where $g(t)$ is a second order polynomial in t and $n = 2k$ or $n = 2k+1$ with $0 \le n \le N_0$.

$$
\begin{aligned}
(e^{g(t)})^{(2k)} &= e^{g(t)}((g'(t))^{2k} + c_1(g'(t))^{2k-2}g''(t) + c_2(g'(t))^{2k-4}(g''(t))^2 \\
&\quad + \cdots + c_k(g''(t))^k) \\
(e^{g(t)})^{(2k+1)} &= e^{g(t)}((g'(t))^{2k+1} + d_1(g'(t))^{2k-1}g''(t) + d_2(g'(t))^{2k-3}(g''(t))^2 \\
&\quad + \cdots + d_k g'(t)(g''(t))^k),
\end{aligned}
$$

where $c_j > 0$, $d_j > 0$, for $j = 1, \dots, k$ are the constants depending only on n and hence on N_0.

Applying the above identities to $g(t) = \frac{1}{2}\alpha t^2$ with $|t| \le 1$ and $|\alpha| \le 1$, we have

$$
\begin{aligned}
(e^{\frac{1}{2}\alpha t^2})^{(2k)} &= e^{\frac{1}{2}\alpha t^2}\left((\alpha t)^{2k} + c_1(\alpha t)^{2k-2}\alpha + c_2(\alpha t)^{2k-4}\alpha^2 + \dots c_k\alpha^k\right) \\
&= c_k\alpha^k e^{\frac{1}{2}\alpha t^2}(1 + \sigma(\alpha,t)\alpha), \\
(e^{\frac{1}{2}\alpha t^2})^{(2k+1)} &= e^{\frac{1}{2}\alpha t^2}\left((\alpha t)^{2k+1} + d_1(\alpha t)^{2k-1}\alpha + c_2(\alpha t)^{2k-3}\alpha^2 + \dots c_k(\alpha t)\alpha^k\right) \\
&= c_k\alpha^{k+1}te^{\frac{1}{2}\alpha t^2}(1 + \beta(\alpha,t)\alpha),
\end{aligned}
$$

where $|\sigma(\alpha,t)| \le K_1$, $|\beta(\alpha,t)| \le K_2$ for all $|t| \le 1$ and $|\alpha| \le 1$ and K_1, K_2 are the constants depending only on n and hence on N_0.

Finally, we define the constant M by $M = \max\{M_1, 2\pi K_1, 2\pi K_2, 16\}$.

We are now ready to state our main results. The first theorem covers the case of regular edge points, while the second theorem covers the case of corner points.

Theorem 3.1. *Let S, B, G and M be defined as above. Assume that $\psi^{(d)}, \psi_M^{(d)} \in L^2(\mathbb{R})$ are given by (2.7), with $d = \mathfrak{h}$ or $d = \mathfrak{v}$, and w, v are defined by (2.5) and (2.6). If $p \in \partial S$, we write $p = (G(u_p), u_p)$ and let $D_k = \frac{d^k}{du^k}(f_G(u))|_{u=u_p}$.*

(i) If $p \notin \partial S$ then, for all $N > 0$,

$$\lim_{a\to 0^+} a^{-N}\,\mathcal{SH}_\psi B(a, s_0, p) = 0 \text{ and } \lim_{a\to 0^+} a^{-N}\,\mathcal{SH}_{\psi_M} B(a, s_0, p) = 0.$$

(ii) If $p \in \partial S$ is a regular point and $s = s_0$ does not correspond to the normal direction of ∂S at p then, for all $N > 0$,

$$\lim_{a\to 0^+} a^{-N}\,\mathcal{SH}_\psi B(a, s_0, p) = 0 \text{ and } \lim_{a\to 0^+} a^{-N}\,\mathcal{SH}_{\psi_M} B(a, s_0, p) = 0.$$

(iii) If $p \in \partial S$ is a regular point, $D_0 \neq 0$ and $s = s_0$ corresponds to the normal direction of ∂S at p then

$$0 < \lim_{a\to 0^+} a^{-\frac{3}{4}}|\mathcal{SH}_\psi B(a, s_0, p)| < \infty \text{ or } 0 < \lim_{a\to 0^+} a^{-\frac{3}{4}}\,\mathcal{SH}_{\psi_M} B(a, s_0, p) < \infty.$$

Otherwise, if $p \in \partial S$ be a regular point, $D_k = 0$ for $1 \le k \le n-1$ and $D_n \neq 0$, where $n \le N_0$, and $s = s_0$ corresponds to the normal direction of ∂S at p then

$$
\begin{aligned}
&0 < \lim_{a\to 0^+} a^{-(\frac{n}{2}+\frac{3}{4})}|\mathcal{SH}_\psi B(a, s_0, p)| < \infty \\
\text{or}\quad &0 < \lim_{a\to 0^+} a^{-(\frac{n}{2}+\frac{3}{4})}|\mathcal{SH}_{\psi_M} B(a, s_0, p)| < \infty.
\end{aligned}
$$

Theorem 3.2. *Let S, B, $\psi^{(d)}$, $\psi_M^{(d)}$ be defined as above. If $p \in \partial S$, we write $p = (G(u_p), u_p)$ and let $D_k^+ = \frac{d^k}{du^k}(f_{G_1}(u))|_{u=u_p^+}$, $D_k^- = \frac{d^k}{du^k}(f_{G_2}(u))|_{u=u_p^-}$.*

(i) If $p \in \partial S$ is a corner point, $D_0^- \neq 0$ or $D_0^+ \neq 0$, and $s = s_0$ does not correspond to any of the normal directions of ∂S at p, then

$$\lim_{a\to 0^+} a^{-\frac{9}{4}} |\mathcal{SH}_\psi B(a, s_0, p)| < \infty \text{ and } \lim_{a\to 0^+} a^{-\frac{9}{4}} |\mathcal{SH}_{\psi_M} B(a, s_0, p)| < \infty.$$

Otherwise, if $p \in \partial S$ is a corner point, $D_k^- = 0$ for $1 \le k \le n_1 - 1$ and $D_{n_1}^- \neq 0$, $D_k^+ = 0$ for $1 \le k \le n_2 - 1$ and $D_{n_2}^+ \neq 0$, where $n_1, n_2 \le N_0$, and $s = s_0$ does not correspond to any of the normal directions of ∂S at p, then

$$\lim_{a\to 0^+} a^{-(n+\frac{9}{4})} |\mathcal{SH}_\psi B(a, s_0, p)| < \infty \text{ and } \lim_{a\to 0^+} a^{-(n+\frac{9}{4})} |\mathcal{SH}_{\psi_M} B(a, s_0, p)| < \infty,$$

where $n = \min\{n_1, n_2\}$.

(ii) Assume that $p \in \partial S$ is a corner point and $s = s_0$ corresponds to the right-side normal direction $\vec{n}(u_p^+)$ of ∂S at p, that $D_k^+ = 0$ for $1 \le k \le n_1 - 1$ and $D_{n_1} \neq 0$ and $D_k^- = 0$ for $1 \le k \le n_2 - 1$ and $D_{n_2} \neq 0$, where $n_1, n_2 \le N_0$.
If $n_2 + \frac{9}{4} > \frac{n_1}{2} + \frac{3}{4}$, then

$$\begin{aligned} & 0 < \lim_{a\to 0^+} a^{-(\frac{n_1}{2}+\frac{3}{4})} |\mathcal{SH}_\psi B(a, s_0, p)| < \infty \\ \text{or} \quad & 0 < \lim_{a\to 0^+} a^{-(\frac{n_1}{2}+\frac{3}{4})} |\mathcal{SH}_{\psi_M} B(a, s_0, p)| < \infty. \end{aligned} \tag{3.2}$$

If $n_2 + \frac{9}{4} \le \frac{n_1}{2} + \frac{3}{4}$, then

$$\begin{aligned} & \lim_{a\to 0^+} a^{-(n_2+\frac{9}{4})} |\mathcal{SH}_\psi B(a, s_0, p)| < \infty \\ \text{and} \quad & \lim_{a\to 0^+} a^{-(n_2+\frac{9}{4})} |\mathcal{SH}_{\psi_M} B(a, s_0, p)| < \infty. \end{aligned} \tag{3.3}$$

If $D_0^+ \neq 0$ or $D_0^- \neq 0$, the estimates (3.2) *and* (3.3) *hold true with $n_1 = 0$ or $n_2 = 0$, respectively.*
If $p \in \partial S$ is a corner point and $s = s_0$ corresponds to the left-side normal direction $\vec{n}(u_p^-)$ of ∂S, then the same estimates hold, with the roles of n_1 and n_2 reversed.

In the situation where $D_0 \neq 0$, the estimates of Theorem 3.1 give the same asymptotic decay rates $O(a^{\frac{3}{4}})$ as the results from [12]. Note, however, that in order to detect the edge we now use two shearlet transforms rather than a single one, as we did in [12] (where we made different assumptions on the shearlet generators). In the situation where $D_0 = 0$, the asymptotic decay rate at a point p on the edge is faster than $O(a^{\frac{3}{4}})$ and the decay rate is increasingly faster as the number of vanishing derivatives D_k at p increases.

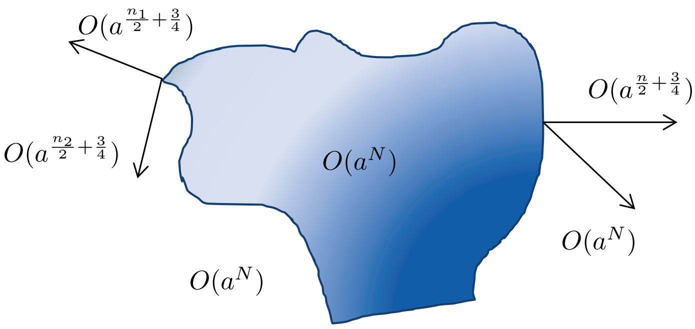

Figure 2: Asymptotic decay of the continuous shearlet transform of $B = f\chi_S$, where f is a smooth function and $S \subset \mathbb{R}^2$ has piecewise smooth boundary. Away from the boundary, the decay is faster than $O(a^N)$, for any $N \in \mathbb{N}$. At the regular points $p \in \partial S$, for normal orientation, the shearlet transform decays as $O(a^{\frac{n}{2}+\frac{3}{4}})$, where n is the order of the first non-vanishing derivative at p; for all other values of s, the decay is faster than $O(a^N)$, for any $N \in \mathbb{N}$. At a corner point p, the shearlet transform decays as $O(a^{\frac{n_1}{2}+\frac{3}{4}})$ and $O(a^{\frac{n_2}{2}+\frac{3}{4}})$ for the two normal orientations corresponding to the 2 curves joining at p; in this case, n_1, n_2 are the orders of the first non-vanishing derivatives at the right- and left-neighborhoods of p (for simplicity, we suppose to be in the case where $n_2 + \frac{9}{4} > \frac{n_1}{2} + \frac{3}{4}$).

According to Theorem 3.2, if p is a corner point and s_0 does not correspond to any of the normal directions, then we only know that the asymptotic decay of $|\mathcal{SH}_\psi B(a, s_0, p)|$ is not slower than $O(a^{(n+\frac{9}{4})})$. However, this estimate cannot be improved as one can follow the argument in [12] to see that the above decay rate is exact (lower bound is not zero) for a corner point of a half disk, but it is not exact (lower bound is zero) for a corner point of a polygon. Also in this case, when $n_1 = n_2 = 0$, the theorem gives the same asymptotic decay as the corresponding result from [12]. The asymptotic decay properties of the shearlet transform in the situation of Theorems 3.1-3.2 are illustrated in Fig. 2.

3.1. Example

The following example is useful to illustrate the application of Theorems 3.1 and 3.2.

Let $S \subset \mathbb{R}^2$ be a polygon, $f(x, y) = Ex + Fy$, for some constants E, F, and, as in the notation of the theorems above, let $B = f\chi_S$.

Each of the finitely many boundary edges of S can be parametrized either as a curve $L_1 = \{(\alpha u + \beta, u);\ u_1 \le u \le u_2\}$ or a curve $L_2 = \{(v, \gamma v + \delta);\ v_1 \le v \le v_2\}$, for some constants $\alpha, \gamma, \delta, \gamma, u_1, u_2, v_1, v_2$. Corresponding to the curves L_1, L_2, let

$$f_1(u) = f(\alpha u + \beta, u) = E(\alpha u + \beta) + Fu = (E\alpha + F)u + E\beta,$$

$$f_2(v) = f(v, \gamma v + \delta) = Ev + F(\gamma v + \delta) = (F\gamma + E)v + F\delta.$$

We notice that the horizontal shearlets can be used deal with L_1 and f_1, and the vertical shearlets with L_2 and f_2. Since the two cases are very similar, we only consider L_1 and f_1 here.

To apply Theorems 3.1 and 3.2 to $B = f\chi_S$ (in the case where we use f_1), we assume that $(E\alpha+F)^2 + (E\beta)^2 > 0$, so that we can guarantee the existence of the constant N_0, as indicated above. If $E\alpha + F = 0$, then $N_0 = 0$ and if $E\alpha + F \neq 0$, then $N_0 = 1$.

Case 1: regular boundary point. Take $p \in \mathbb{R}^2$ to be a regular point on the boundary of the polygon S and suppose that $p = (\alpha u_0 + \beta, u_0)$ for some $u_1 < u_0 < u_2$. Then using Theorems 3.1 we have the following.

(i) If $s = s_0$ does not correspond to the normal direction of ∂S at p then

$$\lim_{a\to 0^+} a^{-N}\, \mathcal{SH}_\psi B(a, s_0, p_0) = 0, \qquad \text{for all } N > 0.$$

(ii) If $(E\alpha + F)u_0 + E\beta \neq 0$ and $s = s_0$ corresponds to the normal direction of ∂S at p_0, then

$$\lim_{a\to 0^+} a^{-\frac{3}{4}}\, \mathcal{SH}_\psi B(a, s_0, p_0) \neq 0.$$

(iii) If $(E\alpha + F)u_0 + E\beta = 0$ (then $E\alpha + F \neq 0$) and $s = s_0$ corresponds to the normal direction of ∂S at p_0 then

$$\lim_{a\to 0^+} a^{-(\frac{1}{2}+\frac{3}{4})}\, \mathcal{SH}_\psi B(a, s_0, p_0) \neq 0.$$

Case 2: corner boundary point. Take $p_c \in \mathbb{R}^2$ to be a corner point on the boundary of the polygon S. In this case, p_c can be identified as $p_c = (\alpha u_1+\beta, u_1)$ corresponding to the endpoint of a segment $L = \{(\alpha u + \beta, u);\ u_1 \leq u \leq u_2\}$. It can also be identified as the endpoint $p_c = (\tilde{\alpha} u_2 + \tilde{\beta}, u_2)$ of another segment $\tilde{L} = \{(\tilde{\alpha} u + \tilde{\beta}, u);\ u_1 \leq u \leq u_2\}$. Below, we consider only one of the two cases, since the other one is similar.

Using Theorems 3.2 we have the following.

(i) If $(E\alpha + F)u_1 + E\beta \neq 0$ and $s = s_0$ does not correspond to any of the normal directions of ∂S at p_c, then

$$\lim_{a\to 0^+} a^{-\frac{9}{4}}\, |\mathcal{SH}_\psi B(a, s_0, p_c)| < \infty.$$

(ii) If $(E\alpha + F)u_1 + E\beta = 0$ and $s = s_0$ does not correspond to any of the normal directions of ∂S at p_c, then

$$\lim_{a\to 0^+} a^{-(1+\frac{9}{4})}\, |\mathcal{SH}_\psi B(a, s_0, p_c)| < \infty.$$

(iii) If $(E\alpha + F)u_1 + E\beta \neq 0$ and $s = s_0$ corresponds to one of the normal directions of ∂S at p_c then

$$0 < \lim_{a\to 0^+} a^{-\frac{3}{4}}\, |\mathcal{SH}_\psi B(a, s_0, p_c)| < \infty.$$

(iv) If $(E\alpha + F)u_1 + E\beta = 0$ and $s = s_0$ corresponds to one of the normal directions of ∂S at p_c then

$$0 < \lim_{a\to 0^+} a^{-(\frac{1}{2}+\frac{3}{4})}\, |\mathcal{SH}_\psi B(a, s_0, p_c)| < \infty.$$

3.2. Organization of the proofs

We will briefly outline the main ideas of the proof, also in comparison with the similar results valid in the case of step edges.

We recall that the original proofs of the edge detection results in [12] (and similarly their 3D extensions [13, 14]) involve the following steps: (i) localization property, to ensure that the asymptotic decay properties of $\mathcal{SH}_\psi B(a, s, p)$, as $a \to 0$, depend only on the behavior of B near p; (ii) divergence theorem, to convert the area integral over the region S into a line integral over ∂S; (iii) quadratic approximation, to locally approximate ∂S using a quadratic curve; (iv) lower bound estimate, to ensure that $\mathcal{SH}_\psi B(a, s, p)$ decays slowly when $p \in \partial S$ and $s = s_0$ corresponds to the normal direction of ∂S. As we mentioned above, the last step is the most delicate and it relies on the method of stationary phase and some special assumptions about the generator ψ (cf. Section 2).

The intuitive idea that we will apply to extend the results from [12] to the situation $B = f\chi_S$, where f is a smooth function, is to locally approximate f with its Taylor expansion, and then try to adapt the old argument using integration by parts. In fact, using this idea, we can handle parts (i) and (ii) of Theorem 3.1. Unfortunately, part (iii) of Theorem 3.1 (the most difficult part of the proof) cannot be handled as easily. As we mentioned above, the difficulty is that we have very little control on f at p (f and its derivatives up to a certain order may vanish at p!) and we cannot adapt the argument from [12] in this case. In the new proof, we will still use the localization property as in the old argument (Lemma 4.2 below), ensuring that the asymptotic decay of $\mathcal{SH}_\psi B(a, s, p)$ depends only on the behavior of B near p. Next, we will use an application of the divergence theorem (Lemma 4.1 below) to convert the integral expression of $\mathcal{SH}_\psi B(a, s, p)$ into a line integral over ∂S. To prove part (iii) of Theorem 3.1, we will introduce a new argument that uses two distinct shearlet systems, one to handle the edge points with curvatures near zero and another one for the edge points with curvature away from zero. The proof of Theorem 3.2 follows a similar structure with the difference that, at the corner points, we need to examine separately the right and left neighbourhoods of the boundary curve.

4. Divergence theorem and localization lemmata

We start by constructing the analytical tools that we need to prove the main theorems of this paper. Lemma 4.1, in particular is an application of the Divergence theorem and Lemmata 4.2 and 4.3 show that the continuous shearlet transform exhibits some useful localization properties.

We start by recalling the classical *Divergence theorem* in $\mathbb{R}^2$.

Let $\vec{F}$ be a smooth vector field on $\mathbb{R}^2$ and $S \in \mathbb{R}^2$ be a compact region with piecewise smooth boundary ∂S. Then

$$\int_S \nabla \cdot \vec{F}\, dA = \int_{\partial S} \vec{F} \cdot \vec{n}\, d\sigma,$$

where $\vec{n}$ is the unit outward normal vector to ∂S, the left-hand side of the equality is the area integral over the region S, the right-hand side is the curvilinear integral over the curve ∂S and σ is the 1-dimensional Hausdorff measure on $\mathbb{R}^2$.

Let $f \in C^\infty(\mathbb{R}^2)$ and, for $\xi \in \mathbb{R}^2$, and let $\vec{F}$ be a smooth vector field on $\mathbb{R}^2$ defined by

$$\vec{F}(x) = (F_1(x), F_2(x)) = e^{-2\pi i \xi \cdot x} f(x)\, \xi.$$

Then the Divergence theorem gives that

$$\int_S e^{-2\pi i \xi \cdot x} \left((-2\pi i)|\xi|^2 f(x) + (\nabla_x f) \cdot \xi \right) dx = \int_{\partial S} e^{-2\pi i \xi \cdot x} f(x)\, \xi \cdot \vec{n}(x)\, d\sigma(x),$$

or

$$\int_S e^{-2\pi i \xi \cdot x} f(x)\, dx = \tfrac{-1}{2\pi i |\xi|^2} \int_{\partial S} e^{-2\pi i \xi \cdot x} f(x)\, \xi \cdot \vec{n}(x) d\sigma(x) + \tfrac{1}{2\pi i |\xi|} \int_S e^{-2\pi i \xi \cdot x} (\nabla_x f) \cdot \tfrac{\xi}{|\xi|} dx.$$

We can apply now the Divergence theorem again to the second integral on the right with $f(x)$ being replaced by $f_1(x) = (\bigtriangledown_x f) \cdot \frac{\xi}{|\xi|}$ to get

$$\begin{aligned} & \tfrac{1}{2\pi i |\xi|} \int_S e^{-2\pi i \xi \cdot x} f_1(x)\, dx \\ & = \tfrac{1}{(2\pi)^2 |\xi|^3} \int_{\partial S} e^{-2\pi i \xi \cdot x} f_1(x)\, \xi \cdot \vec{n}(x)\, d\sigma(x) - \tfrac{1}{(2\pi)^2 |\xi|^2} \int_S e^{-2\pi i \xi \cdot x} (\nabla_x f_1) \cdot \tfrac{\xi}{|\xi|}\, dx. \end{aligned}$$

We can now let $f_2(x) = (\nabla_x f_1) \cdot \frac{\xi}{|\xi|}$ and repeat the above process until we obtain the following result.

Lemma 4.1. *Let $S \in \mathbb{R}^2$ be a compact region with piecewise smooth boundary ∂S and f be a polynomial of two variables of order L. Then there exist constants $c_0, c_1, c_2, \cdots, c_L$ such that*

$$\begin{aligned} & \int_S e^{-2\pi i \xi \cdot x} f(x)\, dx \\ = \; & \tfrac{c_0}{|\xi|} \int_{\partial S} e^{-2\pi i \xi \cdot x} f(x)\, \tfrac{\xi}{|\xi|} \cdot \vec{n}(x)\, d\sigma(x) + \cdots + \tfrac{c_L}{|\xi|^{L+1}} \int_{\partial S} e^{-2\pi i \xi \cdot x} f_L(x)\, \tfrac{\xi}{|\xi|} \cdot \vec{n}(x)\, d\sigma(x) \\ = \; & \sum_{l=0}^{L} \tfrac{c_l}{|\xi|^{l+1}} \int_{\partial S} e^{-2\pi i \xi \cdot x} f_l(x)\, \tfrac{\xi}{|\xi|} \cdot \vec{n}(x)\, d\sigma(x), \end{aligned}$$

where $f_0(x) = f(x)$ and $f_l(x) = (\nabla_x f_{l-1}) \cdot \frac{\xi}{|\xi|}$, for $l = 1, \ldots L$.

We can now apply Lemma 4.1 to simplify the expression of the continuous shearlet transform of $B = f\chi_S$, where f be a polynomial of two variables of order L and S is defined as in Lemma 4.1. Using polar coordinates, we will write $x \in \mathbb{R}^2$ as $x = \rho(\cos\theta, \sin\theta)$, where $\rho \geq 0$ and $\theta \in [0, 2\pi)$. Let $\Theta(\theta) = (\cos\theta, \sin\theta)$. Observing that $\hat{B}(\xi) = \int_S e^{-2\pi i \xi \cdot x} f(x)\, dx$, we then obtain the following identity.

$$\begin{aligned}\mathcal{SH}_\psi B(a,s_0,p) &= \langle B, \psi^{(d)}_{as_0p}\rangle \\ &= \int_0^{2\pi}\int_0^\infty \hat{B}(\rho,\theta)\,\overline{\hat{\psi}^{(d)}_{as_0p}}(\rho,\theta)\,\rho\,d\rho\,d\theta \\ &= \sum_{l=0}^{L} c_l\, I(a,s_0,p,l),\end{aligned}$$

where the upper-script in $\psi^{(d)}_{as_0p}$ is either $d=\mathfrak{h}$, when $|s_0|\le 1$, or $d=\mathfrak{v}$, when $|s_0|>1$, and where

$$\begin{aligned}&I(a,s_0,p,l)\\ &= \int_0^{2\pi}\int_0^\infty \frac{1}{\rho^l}\int_{\partial S}\overline{\hat{\psi}^{(d)}_{as_0p}}(\rho,\theta)e^{-2\pi i\rho\,\Theta(\theta)\cdot x}\,\Theta(\theta)\cdot\vec{n}(x)\,f_l(x)d\sigma(x)\,d\rho\,d\theta. \quad (4.1)\end{aligned}$$

For $\epsilon>0$, let $D_\epsilon(p)$ be the ball in $\mathbb{R}^2$ of radius ϵ and center p, and $D^c_\epsilon(p) = \mathbb{R}^2\setminus D_\epsilon(p)$. Hence, we can split the integral (4.1) as

$$I(a,s_0,p,l) = I_1(a,s_0,p,l) + I_2(a,s_0,p,l),$$

where

$$\begin{aligned}&I_1(a,s_0,p,l)\\ &= \int_0^{2\pi}\int_0^\infty \tfrac{1}{\rho^l}\int_{\partial S\cap D_\epsilon(p)}\overline{\hat{\psi}^{(d)}_{as_0p}}(\rho,\theta)e^{-2\pi i\rho\,\Theta(\theta)\cdot x}\Theta(\theta)\cdot\vec{n}(x)\,f_l(x)\,d\sigma(x)\,d\rho\,d\theta; \quad (4.2)\\ &I_2(a,s_0,p,l)\\ &= \int_0^{2\pi}\int_0^\infty \tfrac{1}{\rho^l}\int_{\partial S\cap D^c_\epsilon(p)}\overline{\hat{\psi}^{(d)}_{as_0p}}(\rho,\theta)e^{-2\pi i\rho\,\Theta(\theta)\cdot x}\Theta(\theta)\cdot\vec{n}(x)\,f_l(x)\,d\sigma(x)\,d\rho\,d\theta. \quad (4.3)\end{aligned}$$

The following lemma shows that the integral I_2 exhibits rapid asymptotic decay as $a\to 0$. In other words, the asymptotic decay of the shearlet transform $\mathcal{SH}_\psi B(a,s_0,p)$, as $a\to 0$, is only determined by the values of the boundary ∂S which are close to p. The proof of this lemma is the same as Lemma 4.1 in [12] and is omitted.

Lemma 4.2. *Let $I_2(a,s_0,p,l)$ be given by (4.3). For any $N\in\mathbb{N}$, there is a constant $C_N>0$ such that, for $a<1$, we have*

$$|I_2(a,s_0,p,l)| \le C_N\, a^N,$$

uniformly for all $s_0\in\mathbb{R}$, $p\in S$ and $0\le l\le L$.

The following lemma shows that we can approximate the shearlet transform of $B_f = f\chi_S$, where $f\in C^\infty$, using the shearlet transform of $B_f = P\chi_S$, where P is an appropriate polynomial. Our proof below is similar to the proof of Lemma 4.2 in [12].

Lemma 4.3. *Given $f \in C^\infty(\mathbb{R}^2)$, let $P_{L,p}$ be its Taylor polynomial of order L centered at $p \in \mathbb{R}^2$. Let $B_f = f\chi_S$ and $B_{L,p} = P_{L,p}\chi_S$. For any $s_0 \in \mathbb{R}$, $a < 1$, there is a constant C_L such that*

$$|\mathcal{SH}_\psi B_f(a, s_0, p) - \mathcal{SH}_\psi B_{L,p}(a, s_0, p)| \le C_L\, a^{\frac{L-1}{4}}.$$

Proof. Without loss of generality, we may assume $s = 0$. We use the notation $x = (x_1, x_2) \in \mathbb{R}^2$.

A direct calculation shows that

$$\begin{aligned} |\mathcal{SH}_\psi B_f(a, 0, p) - \mathcal{SH}_\psi B_{L,p}(a, 0, p)| &\le \int_{\mathbb{R}^2} |\psi_{a0p}(x)|\, |f(x) - P_{L,p}(x)|\, \chi_S(x)\, dx \\ &= T_1(a) + T_2(a), \end{aligned}$$

where, for $x = (x_1, x_2)$, we have:

$$\begin{aligned} T_1(a) &= a^{-\frac{3}{4}} \int_{D(a^{\frac{1}{4}},p)} |\psi(a^{-1}x_1, a^{-\frac{1}{2}}x_2)|\, |f(x) - P_{L,p}(x)| \chi_S(x)\, dx_1\, dx_2; \\ T_2(a) &= a^{-\frac{3}{4}} \int_{D^c(a^{\frac{1}{4}},p)} |\psi(a^{-1}x_1, a^{-\frac{1}{2}}x_2)|\, |f(x) - P_{L,p}(x)| \chi_S(x)\, dx_1\, dx_2. \end{aligned}$$

A straightforward calculation shows that

$$T_1(a) \le C\, a^{-\frac{3}{4}} \int_{D(a^{\frac{1}{4}},p)} |f(x) - P_{L,p}(x)| \chi_S(x)\, dx_1\, dx_2 \le C_L a^{\frac{1}{4}(L+2)-\frac{3}{4}}. \quad (4.4)$$

It remains to control $T_2(a)$. The assumptions on ψ imply that, for each $N > 0$, there is a constant $C_N > 0$ such that $|\psi(x)| \le C_N\, (1 + |x|^2)^{-N}$. Thus, for $a < 1$, we can estimate $T_2(a)$ as:

$$\begin{aligned} T_2(a) &\le C\, a^{-\frac{3}{4}} \int_{D^c(a^{\frac{1}{4}},p)} |\psi(a^{-1}x_1, a^{-\frac{1}{2}}x_2)|\, dx_1\, dx_2 \\ &\le C_N\, a^{-\frac{3}{4}} \int_{D^c(a^{\frac{1}{4}},p)} \Big(1 + (a^{-1}x_1)^2 + (a^{-\frac{1}{2}}x_2)^2\Big)^{-N} dx_1\, dx_2 \\ &\le C_N\, a^{-\frac{3}{4}} \int_{D^c(a^{\frac{1}{4}},p)} \Big((a^{-1/2}x_1)^2 + (a^{-\frac{1}{2}}x_2)^2\Big)^{-N} dx_1\, dx_2 \\ &= C_N\, a^{N-\frac{3}{4}} \int_{D^c(a^{\frac{1}{4}},p)} \big(x_1^2 + x_2^2\big)^{-N} dx_1\, dx_2 \\ &= C_N\, a^{N-\frac{3}{4}} \int_{a^{\frac{1}{4}}}^{\infty} r^{-1-2N}\, dr \\ &\le C_N\, a^{2N(\frac{1}{2}-\frac{1}{4})+2\frac{1}{4}-\frac{3}{4}} \le C_N a^{\frac{N}{2}-\frac{1}{4}}. \end{aligned} \quad (4.5)$$

The proof follows from (4.4) and (4.5). ☐

5. Proofs of the main results

We can now prove the main theorems of the paper.

5.1. Proof of Theorem 3.1

By Lemma 4.3, in order to estimate the continuous shearlet transform of $\mathcal{SH}_\psi B(a,s,p)$, where $B = f\chi_S$, we can locally approximate the C^∞ function f near p using a polynomial of order L, resulting in an error of order a^{-L+1}, for a small. Thus, in the following, we can assume that f is a polynomial of order L, for L large enough. With this observation, we can now apply Lemma 4.1 so that, in order to obtain the estimates stated by the theorem, it will be sufficient to estimate the integrals (4.1).

In the proof below, to estimate the integrals (4.1) we can split the integral with respect to θ into the interval $|\theta_0| \le \frac{\pi}{4}$ and its complement. In the following we will only consider the case $|\theta_0| \le \frac{\pi}{4}$, corresponding to the situation where the shearlet transform is associated with the horizontal shearlets $\{\psi_{asp}^{(\mathfrak{h})}\}$. Clearly, for the case $\frac{\pi}{4} < |\theta_0| \le \frac{\pi}{2}$, we can use the shearlet transform associated with the vertical shearlets. The analysis of this second case is very similar to the first case and is omitted. To simplify notation, in the following, we will drop the upper script $\mathfrak{h}$ and simply write ψ and ψ_M for $\psi^{(\mathfrak{h})}$ and $\psi_M^{(\mathfrak{h})}$.

In parts (i) and (ii) of the proof, we only consider the shearlet transform $\mathcal{SH}_\psi B$ with generator ψ. When ψ is replaced by ψ_M, the argument is the same.

Proof of (i). The proof of this statement follows directly from Lemma 4.2 since, in this case, $p \notin \partial S$ and, thus, to estimate the integrals (4.1) we only need to consider the terms $I_2(a, s_0, p, l)$, for $l = 0, \dots L$.

Proof of (ii). Again, due to Lemma 4.2, since $p \in \partial S$ we need to consider only the terms $|I_1(a, s_0, p, l)|$ for $l = 0, \dots L$. Without loss of generality, we may assume $p = (0,0)$ and $\theta_0 = 0$ so that $s_0 = 0$. Under the assumption that $p = (0,0)$ is a regular point of ∂S, we can write that $\partial S \cap D_\epsilon(0) = \{(G(u), u) \colon u \in U\}$, where U is a small neighborhood of $u = 0$ and $G(u)$ is a smooth function such that $G(0) = G'(0) = 0$ (by a linear change of coordinate if necessary), so that $G(u) = Au^2 + O(u^3)$ for all $u \in U$, where A is a constant that depends on the curvature of ∂S at p.

Due to the hypothesis that s_0 does not correspond to the normal direction of ∂S at p, we have that $\Theta(\theta_0) \neq \pm\vec{n}(p)$. Since the tangent line to ∂S at p is generated by the tangent vector $(G'(0), 1) = (0, 1)$ (so that $\vec{n}(p) = (1, 0)$), we must have that $\Theta(\theta_0) \cdot (0,1) \neq 0$.

From (4.2), using the fact that $\hat{\psi}_{a00}^{(\mathfrak{h})}(\rho,\theta) = a^{\frac{3}{4}} w(a\rho\cos\theta) v(a^{-\frac{1}{2}}\tan\theta)$, the parametrization $\{(G(u), u) \colon u \in U\}$ for the arc segment $\partial S \cap D_\epsilon(0)$ and the change of variable $a\rho \to \rho$, we obtain:

$$\begin{aligned} I_1(a,0,0,l) &= a^{\frac{3}{4}} \int_0^{2\pi}\int_0^{\infty} \tfrac{1}{\rho^l} w(a\rho\cos\theta) v(a^{-\frac{1}{2}}\tan\theta) \\ &\times \int_U e^{-2\pi i\rho\,\Theta(\theta)\cdot(G(u),u)}\Theta(\theta)\cdot(-1,G'(u))\, f_l((G(u),u))\,du\,d\rho\,d\theta \\ &= a^{l-\frac{1}{4}} \int_0^{2\pi}\int_0^{\infty} \tfrac{1}{\rho^l} w(\rho\cos\theta) v(a^{-\frac{1}{2}}\tan\theta) \\ &\times \int_U e^{-2\pi i\frac{\rho}{a}\,\Theta(\theta)\cdot(G(u),u)}\Theta(\theta)\cdot(-1,G'(u))\, f_l(G(u),u)\,du\,d\rho\,d\theta \end{aligned}$$

Note that the domain of integration of U is arbitrarily small near $p = 0$. Let $F \in C_c^\infty(U)$ be a bump function satisfying the condition that $F(u) = 1$ for all u in a sufficiently small compact subset of U. Next, we write $I_1(a,0,0,l)$, given by the last equation, as

$$I_1(a,0,0,l) = I_{11}(a,0,0,l) + I_{12}(a,0,0,l),$$

where, for $j = 1,2$,

$$I_{1j}(a,0,0,l) = a^{l-\frac{1}{4}} \int_0^{2\pi}\int_0^{\infty} \tfrac{1}{\rho^l} w(\rho\cos\theta) v(a^{-\frac{1}{2}}\tan\theta)\, K_j(\rho,\theta)\,d\rho\,d\theta,$$

and

$$K_1(\rho,\theta) = \int_U F(u) e^{-2\pi i\frac{\rho}{a}\,\Theta(\theta)\cdot(G(u),u)}\Theta(\theta)\cdot(-1,G'(u))\, f_l(G(u),u)\,du,$$

$$K_2(\rho,\theta) = \int_U (1-F(u)) e^{-2\pi i\frac{\rho}{a}\,\Theta(\theta)\cdot(G(u),u)}\Theta(\theta)\cdot(-1,G'(u))\, f_l(G(u),u)\,du.$$

The rest of the argument is now identical to the one of part(ii) of Theorem 1.1 from [12]. Namely, we observe that, for U sufficiently small we have that, for all $\theta \in [-\frac{\pi}{4}, \frac{\pi}{4}]$ and $u \in U$, $\Theta(\theta)\cdot(G'(u),1) \neq 0$. Hence, we can integrate by parts K_1 with respect to u repeatedly. This shows that, for any positive integer N, there is a positive constant $C_{N,m}$ such that $|I_1(a,0,0,l)| \le C_{N,l} a^N$. Since there are only finite l, there is a positive constant C_N such that $|I_1(a,0,0)| \le C_N a^N$. This proves (ii).

Proof of (iii). As in part (ii), due to Lemma 4.2, we need to consider only the terms $|I_1(a,s_0,p,l)|$ for $l = 0,\dots M$. Again, we assume $p = (0,0)$ and $\theta_0 = 0$ so that $s_0 = 0$; also, we write that $\partial S \cap D_\epsilon(0) = \{(G(u),u) : u \in U\}$, where U is a small neighborhood of $u = 0$ and $G(u)$ is a smooth function such that $G(0) = G'(0) = 0$ (by a linear change of coordinate if necessary), so that $G(u) = Au^2 + O(u^3)$ for all $u \in U$, where A is a constant that depends on the curvature of ∂S at p.

Due to the hypothesis that s_0 corresponds to the normal direction of ∂S at p, we have that $\Theta(\theta_0) = \pm\vec{n}(p)$.

We will only need to examine $I_1(a,0,0,l)$ for $l=0$. As the proof below will show, the integrals $I_1(a,0,0,l)$ for $l>0$ yield higher order decay rate as $a \to 0$.

We start by considering the continuous shearlet transform with generator ψ. Recall that $\hat{\psi}^{(\mathfrak{h})}_{a00}(\rho,\theta) = a^{\frac{3}{4}} w(a\rho\cos\theta) v(a^{-\frac{1}{2}}\tan\theta)$. Hence, with the change of variable $a\rho \to \rho$, from (4.2), we obtain

$$I_1(a,0,0,0) = a^{-\frac{1}{4}} \int_0^{2\pi}\int_0^{\infty} w(\rho\cos\theta) v(a^{-\frac{1}{2}}\tan\theta)$$
$$\times \int_U e^{-2\pi i \frac{\rho}{a}\Theta(\theta)\cdot(G(u),u)} f(G(u),u)\,\Theta(\theta)\cdot(-1,G'(u))du\,d\rho\,d\theta. \quad (5.1)$$

In the following, for the given n with $0 \le n \le N_0$ in the assumption of (iii), we will show that

$$\lim_{a\to 0^+} a^{-(\frac{n}{2}+\frac{3}{4})} I_1(a,0,0,0) \neq 0.$$

To analyze the integral I_1, we replace the interval of integration $[0,2\pi]$ for θ with the (equivalent) interval $[-\frac{\pi}{2},\frac{3\pi}{2}]$ and split $[-\frac{\pi}{2},\frac{3\pi}{2}]$ into $[-\frac{\pi}{2},\frac{\pi}{2}] \cup [\frac{\pi}{2},\frac{3\pi}{2}]$. Using the change of variable $\theta = \theta' + \pi$ for the integral on $[\frac{\pi}{2},\frac{3\pi}{2}]$ and using the fact that w is odd, we can write I_1 as

$$I_1(a,0,0,0) = I_{11}(a,0,0,0) + I_{12}(a,0,0,0), \quad (5.2)$$

where, for $j=1,2$,

$$I_{1j}(a,0,0,0) = a^{-\frac{1}{4}} \int_0^{\infty}\int_{-\frac{\pi}{2}}^{\frac{\pi}{2}} w(\rho\cos\theta)\, v(a^{-1/2}\tan\theta)\, K_j(a,\rho,\theta)\, d\theta\, d\rho,$$

and

$$K_1(a,\rho,\theta) = \int_U e^{-2\pi i \frac{\rho}{a}\Theta(\theta)\cdot(G(u),u)} f(G(u),u)\,\Theta(\theta)\cdot(-1,G'(u))du,$$
$$K_2(a,\rho,\theta) = \int_U e^{2\pi i \frac{\rho}{a}\Theta(\theta)\cdot(G(u),u)} f(G(u),u)\,\Theta(\theta)\cdot(-1,G'(u))du.$$

According to the observation we made at the beginning of the proof (part (iii)), we can write:

$$\frac{1}{a}\Theta(\theta)\cdot(G(u),u) = \cos\theta\left(\frac{1}{a}(Au^2 + O(u^3)) + a^{-\frac{1}{2}}\tan\theta a^{-\frac{1}{2}}u\right).$$

By the hypothesis on f and its derivatives at p, we can write $f(G(u),u)$ as $K_n u^n + O(u^{n+1})$, where K_n is a non-zero constant (note that $0 \le n \le N_0$). Since K_n does not play any role in the proof, without loss of generality, in the following we will assume that $K_n = 1$.

Recall that the function v is supported in $[-1,1]$. It follows that, for the integral I_1, given by (5.1), to be non-zero, we need to satisfy the support restriction $|a^{-1/2}\tan\theta| \le 1$. This implies that, if $a \to 0$, then $\theta \to 0$. Now, let

$a^{-\frac{1}{2}}\tan\theta = t$ and $a^{-\frac{1}{2}}u = y$; then we have the following:

$$
\begin{aligned}
& \lim_{a\to 0^+} a^{-(\frac{n}{2}+\frac{3}{4})}(2\pi i)^n\, I_{11}(a,0,0,0) \\
= \;& (2\pi i)^n \int_{-\infty}^{\infty}\int_0^{\infty}\int_{-1}^{1} e^{-2\pi i\rho(Ay^2+ty)} y^n w(\rho)\, v(t)\, dt d\rho\, dy \\
= \;& \int_{-\infty}^{\infty}\int_0^{\infty}\int_{-1}^{1} e^{-2\pi i\rho(Ay^2+ty)} \rho^{-n} w(\rho)\, v^{(n)}(t)\, dt\, d\rho\, dy \\
= \;& \int_{-1}^{1}\int_0^{\infty} e^{\pi i\rho\frac{1}{2A}t^2}\rho^{-n} w(\rho)\, v^{(n)}(t) \left(\int_{-\infty}^{\infty} e^{-2\pi i\rho A(y+\frac{t}{2A})^2}dy\right) d\rho\, dt \\
= \;& \frac{1}{\sqrt{4A}}(1-i)\int_{-1}^{1}\int_0^{\infty} e^{\pi i\rho\frac{1}{2A}t^2}\rho^{-n-\frac{1}{2}} w(\rho)\, v^{(n)}(t) d\rho\, dt \\
= \;& (-1)^n\frac{1}{\sqrt{4A}}(1-i)\int_{-1}^{1}\int_0^{\infty}\frac{d^n}{dt^n}\left(e^{\pi i\rho\frac{1}{2A}t^2}\right)\rho^{-n-\frac{1}{2}} w(\rho)\, v(t)\, d\rho\, dt \\
:= \;& T_n(A),
\end{aligned}
$$

where we have applied integration by parts with respect to t in the second equation and we have used the identity $\int_{-\infty}^{\infty} e^{-i\frac{\pi}{2}u^2}du = 1-i$ in the fourth equation.

It is easy to verify that, since $w \in C_c^\infty([0,1])$ and $v(t) = e^{t-\frac{1}{1-t^2}}$, then $|T_n(A)| < \infty$ for any A and for all $n = 0,1,2,\ldots,N_0$.

Since w is odd, similarly we have that

$$\lim_{a\to 0^+} a^{-(\frac{n}{2}+\frac{3}{4})}\,(2\pi i)^n\, I_{12}(a,0,0,0) = \overline{T_n}(A).$$

It follows that, in order to show that $\lim_{a\to 0^+} a^{-(\frac{n}{2}+\frac{3}{4})} I_1(a,0,0,0) \neq 0$, it is enough to show that $\mathrm{Real}(T_n(A)) \neq 0$.

A direct calculation shows that

$$
\begin{aligned}
T_n'(A) &= (2\pi i)^n \int_{-\infty}^{\infty}\int_0^{\infty}\int_{-1}^{1} e^{-2\pi i\rho(Ay^2+ty)} y^{n+2} w(\rho)\,\rho\, v(t)\, dt\, d\rho\, dy \\
&= (2\pi i)^n \int_{-\infty}^{\infty}\int_0^{\infty}\rho\, w(\rho)\left(\int_{-1}^{1} e^{-2\pi i\rho y t}\check{v}(t)dt\right) e^{-2\pi i\rho Ay^2} d\rho\, y^{n+2}dy \\
&= (2\pi i)^n \int_{-\infty}^{\infty}\int_0^{\infty}\rho\, w(\rho)\check{v}(-\rho y) e^{-2\pi i\rho Ay^2} d\rho\, y^{n+2}dy \\
&= (-1)^n(2\pi i)^n \int_{-\infty}^{\infty}\int_0^{\infty}\rho^{-(n+2)} w(\rho) e^{-2\pi i A\rho^{-1}u^2} d\rho\,\check{v}(u)\, u^{n+2}du.
\end{aligned}
$$

It follows that

$$|T_n'(A)| \leq (2\pi)^n\left(\int_{-\infty}^{\infty}|\check{v}(u)||u^{n+2}|\,du\right)\left(\int_0^1 w(\rho)\rho^{-(n+2)}d\rho\right) := C_n, \tag{5.3}$$

where C_n is a finite quantity independent of A and dependent only on w, w and n. By taking the maximum over all $0 \leq n \leq N_0$, we define the constant

$$C_{\mathrm{MAX}} = \max\{C_n, 0 \leq n \leq N_0\}. \tag{5.4}$$

For $A=0$, we observe that

$$
\begin{aligned}
T_n(0) = (2\pi i)^n \int_{-\infty}^{\infty}\int_0^{\infty} \left(\int_{-1}^{1} e^{-2\pi i\rho y t} v(t)\, dt\right) w(\rho)\, y^n\, d\rho\, dy \\
&= (2\pi i)^n \int_0^{\infty} \left(\int_{-\infty}^{\infty} \check{v}(-\rho y)\, y^n\, dy\right) w(\rho)\, d\rho \\
&= (-2\pi i)^n \int_0^{\infty} \left(\int_{-\infty}^{\infty} \check{v}(u)\, u^n du\right) w(\rho)\, \rho^{-(n+1)} d\rho \\
&= v^{(n)}(0) \int_0^{\infty} w(\rho)\, \rho^{-(n+1)} d\rho \\
&= e^{-1} \int_0^{1} w(\rho)\, \rho^{-(n+1)} d\rho > 0,
\end{aligned}
$$

where we have used the fact that $w>0$ on $[0,1]$ and that $v(t)=e^{t-\frac{1}{1-t^2}}$, so that $v^{(n)}(0)=e^{-1}$.

From the above expression, it is clear that $T_{n_1}(0) < T_{n_2}(0)$, if $n_1 < n_2$. By (5.3), using the Mean Value theorem, we observe that $|T_n(A)-T_n(0)| \le C_{\text{MAX}}|A|$, where C_{MAX} is given by (5.4), and hence $|\text{Real}(T_n(A)-T_n(0))| \le C_{\text{MAX}}|A|$ for all $n=0,1,\ldots,N_0$. Thus, we have that $\text{Real}(T_n(A)) \ge \frac{1}{2}T_n(0)$ for $|A| \le \frac{T_0(0)}{2C_{\text{MAX}}}$. It is easy to verify that M_1, given by (3.1), satisfies $M \ge M_1 \ge \frac{2C_{\text{MAX}}}{T_0(0)}$. Hence, for $|A| \le \frac{1}{M}$, we have that

$$
\text{Real}(T_n(A)) \ge \frac{1}{2}T_n(0) > 0, \qquad \text{for } n=0,1,\ldots,N_0.
$$

On the other hand, for $|A| \ge \frac{1}{M}$, we shall consider the second shearlet transform defined with the sharlet generator ψ_M, given by (2.7). Let us re-examine the expression of $T_n(A)$ with this different choice of shearlet generator. Since $T_n(-|A|) = \overline{T_n}(|A|)$, we may assume $A>0$. Then, using the identity $\int_{-\infty}^{\infty} e^{-i\frac{\pi}{2}u^2} du = 1-i$, we observe that

$$
\begin{aligned}
& T_n(A) \\
&= (-1)^n \frac{1-i}{2\sqrt{A}} \int_{-1}^{1}\int_0^{\frac{1}{M^2}} \frac{d^n}{dt^n}[e^{\pi i\rho\frac{1}{2A}t^2}]\, \rho^{-(n+\frac{1}{2})} e^{-(\frac{1}{M^2\rho}+\frac{1}{1-M^2\rho})} e^{t-\frac{1}{1-t^2}}\, d\rho\, dt \\
&= (-1)^n M^{2n-1} \frac{1-i}{2\sqrt{A}} \int_{-1}^{1}\int_0^{1} \frac{d^n}{dt^n}[e^{\pi i\rho\frac{1}{2AM^2}t^2}]\, \rho^{-(n+\frac{1}{2})} e^{-(\frac{1}{\rho}+\frac{1}{1-\rho})} d\rho\, e^{t-\frac{1}{1-t^2}}\, dt.
\end{aligned}
$$

Observing that $\frac{1}{|A|M^2} \le \frac{1}{|A|M}\frac{1}{M} \le \frac{1}{M} < \frac{1}{16}$, the calculation we gave for the definition of M with $\alpha = \pi i\rho\frac{1}{AM^2}$ shows that

$$
\begin{aligned}
\frac{d^{2k}}{dt^{2k}}[e^{\pi i\rho\frac{1}{2AM^2}t^2}] &= c_k e^{\pi i\rho\frac{1}{2AM^2}t^2} (\pi i\rho\frac{1}{AM^2})^k \left(1+\sigma(\pi i\rho\frac{1}{AM^2},t)\pi i\rho\frac{1}{AM^2}\right), \\
\frac{d^{2k+1}}{dt^{2k+1}}[e^{\pi i\rho\frac{1}{2AM^2}t^2}] &= d_k e^{\pi i\rho\frac{1}{2AM^2}t^2} (\pi i\rho\frac{1}{AM^2})^{k+1} t \left(1+\beta(\pi i\rho\frac{1}{AM^2},t)\pi i\rho\frac{1}{AM^2}\right).
\end{aligned}
$$

Since $0 \leq \rho \leq 1$, from the definition of M, we observe that

$$|\sigma(\pi i\rho \frac{1}{AM^2}, t)\pi i\rho \frac{1}{AM^2}| \leq \frac{1}{2} |\beta(\pi i\rho \frac{1}{AM^2}, t)\pi i\rho \frac{1}{AM^2}| \leq \frac{1}{2}.$$

It follows that, in order to show that $\text{Real}(T_n(A)) \neq 0$, we can replace $\frac{d^n}{dt^n}(e^{\pi i\rho \frac{1}{2AM^2}t^2})$ by $c_k e^{\pi i\rho \frac{1}{2AM^2}t^2}(\pi i\rho \frac{1}{AM^2})^k$, for $n = 2k$, and similarly by the quantity $d_k e^{\pi i\rho \frac{1}{2AM^2}t^2} t\,(\pi i\rho \frac{1}{AM^2})^{k+1}$, for $n = 2k+1$. We will examine these two cases separately.

Case 1: $n = 2k$. In this case, using the substitution indicated above, we have that

$$T_{2k}(A) = c_k \frac{1}{2\sqrt{A}} i^k M^{4k-1} (\frac{\pi}{2M^2})^k (1-i)(\alpha(A) + \beta(A)i),$$

where

$$\begin{aligned}
\alpha(A) &= \int_{-1}^{1} \left(\int_0^1 \cos(\pi i\rho \frac{1}{2AM^2}t^2)\, \rho^{-(k+\frac{1}{2})}\, e^{-(\frac{1}{\rho}+\frac{1}{1-\rho})} d\rho \right) e^{t-\frac{1}{1-t^2}}\, dt, \\
\beta(A) &= \int_{-1}^{1} \left(\int_0^1 \sin(\pi i\rho \frac{1}{2AM^2}t^2)\, \rho^{-(k+\frac{1}{2})}\, e^{-(\frac{1}{\rho}+\frac{1}{1-\rho})} d\rho \right) e^{t-\frac{1}{1-t^2}}\, dt.
\end{aligned}$$

Since $AM^2 \geq AM \geq 1$ and since $\cos x > \sin x > 0$ for $x \in (0, \frac{\pi}{2})$, it follows that $\alpha(A) > \beta(A) > 0$. Hence, it is easy to see that, when k is even,

$$T_{2k}(A) = C_1 \left(\alpha(A) + \beta(A) + i(\alpha(A) - \beta(A))\right)$$

where $C_1 \neq 0$ and, similarly, when k is odd,

$$T_{2k}(A) = C_2 \left(\alpha(A) - \beta(A) + i(\alpha(A) + \beta(A))\right)$$

where $C_2 \neq 0$. It follows that $\text{Real}(T_n(A)) \neq 0$.

Case 2: $n = 2k+1$. In this case, using the other substitution indicated above, we have that

$$T_{2k+1}(A) = d_k M^{2k+1} \frac{1}{2\sqrt{A}} (\pi\rho \frac{1}{AM^2})^{k+1} (1-i) i^{k+1} (\alpha(A) + i\beta(A)),$$

where

$$\begin{aligned}
\alpha(A) &= \int_{-1}^{1} \left(\int_0^1 \cos(\pi i\rho \frac{1}{2AM^2}t^2)\, \rho^{-(k+\frac{1}{2})}\, e^{-(\frac{1}{\rho}+\frac{1}{1-\rho})} d\rho \right) e^{t-\frac{1}{1-t^2}}\, t\, dt \\
&= \int_{0}^{1} \left(\int_0^1 \cos(\pi i\rho \frac{1}{2AM^2}t^2)\, \rho^{-(k+\frac{1}{2})}\, e^{-(\frac{1}{\rho}+\frac{1}{1-\rho})} d\rho \right) e^{-\frac{1}{1-t^2}}\, (e^t - e^{-t})\, t\, dt; \\
\beta(A) &= \int_{-1}^{1} \left(\int_0^1 \sin(\pi i\rho \frac{1}{2AM^2}t^2)\, \rho^{-(k+\frac{1}{2})}\, e^{-(\frac{1}{\rho}+\frac{1}{1-\rho})} d\rho \right) e^{t-\frac{1}{1-t^2}}\, t\, dt \\
&= \int_{0}^{1} \left(\int_0^1 \sin(\pi i\rho \frac{1}{2AM^2}t^2)\, \rho^{-(k+\frac{1}{2})}\, e^{-(\frac{1}{\rho}+\frac{1}{1-\rho})} d\rho \right) e^{-\frac{1}{1-t^2}}\, (e^t - e^{-t})\, t\, dt.
\end{aligned}$$

As for the above case $n = 2k$, one can verify that $\alpha(A) > \beta(A) > 0$. Similarly, we have that, when k is even,

$$T_{2k+1}(A) = C_1 \left(\alpha(A) - \beta(A) + i(\alpha(A) + \beta(A))\right),$$

where $C_1 \neq 0$ and, when k is odd,

$$T_{2k+1}(A) = C_2 \left(\alpha(A) + \beta(A) + i(\alpha(A) - \beta(A))\right),$$

where $C_2 \neq 0$. It follows that also for $|A| \geq \frac{1}{M}$, using the second type of continuous shearlet transform, we have $\mathrm{Real}(T_n(A)) \neq 0$.

This completes the proof of Theorem 3.1.

5.2. Proof of Theorem 3.2

As in the proof of Theorem 3.1, due to Lemma 4.2, we need to consider only the terms $|I_1(a, s_0, p, l)|$, given by (4.2), for $l = 0, \ldots L$, and it is sufficient to examine the shearlet transform associated with the horizontal shearlets. Without loss of generality, we assume that $p = (0, 0)$ and that the boundary curve ∂S is represented as $\partial S = \{(G_1(u), u) : 0 \leq u < \epsilon\} \cup \{(G_2(u), u) : -\epsilon < u \leq 0\}$ near $u = 0$, where G_1, G_2 are smooth functions. As in the proof of Theorem 3.1, we only need to examine the horizontal shearlet system and we drop the upper-script $\mathfrak{h}$ to simplify notation.

Proof of (i): This part of the proof is similar to the proof of part (i) of Theorem 3.2 in [12]. We will only indicate the modifications that are needed to adapt the argument of the old proof. Note that this proof does not depend on the choice of the shearlet generator ψ or ψ_M in the shearlet transform. We will assume that ψ is the generator. The same conclusion will hold for ψ_M.

We may assume $n_1 > 0, n_2 > 0$. The discussion for $n_1 = 0$ or $n_2 = 0$ is similar. As in the proof of part (ii) of Theorem 3.1, we write

$$\begin{aligned} I_1(a, 0, 0, l) &= a^{l-\frac{1}{4}} \int_0^{2\pi} \int_0^{\infty} \tfrac{1}{\rho^l} w(\rho \cos\theta) v(a^{-\frac{1}{2}} \tan\theta) \\ &\times \int_U e^{-2\pi i \frac{\rho}{a} \Theta(\theta)\cdot(G(u),u)} \Theta(\theta)\cdot(-1, G'(u))\, f_l(G(u), u)\, du\, d\rho\, d\theta, \end{aligned}$$

where now, however, we can split the integral over U into the two sets $(-\epsilon, 0] \cup [0, \epsilon)$ and use the parametrizations $(G_1(u), u)$ if $u \in [0, \epsilon)$ and $(G_2(u), u)$ if $u \in (-\epsilon, 0]$. Next, we apply the product rule to the function $f(G_1(u), u)\, \frac{\Theta(\theta)\cdot\vec{n}(u)}{\Theta(\theta)\cdot\vec{\alpha}'(u)}$ on $[0, \epsilon)$ and to the function $f(G_2(u), u)\, \frac{\Theta(\theta)\cdot\vec{n}(u)}{\Theta(\theta)\cdot\vec{\alpha}'(u)}$ on $(-\epsilon, 0]$. Now, we observe that $\frac{d^k}{du^k}(f(G_1(u), u))|_{u=0^+} = 0$ for $0 \leq k \leq n_1 - 1$, $\frac{d^{n_1}}{du^{n_1}}(f(G_1(u), u))|_{u=0^+} \neq 0$, $\frac{d^k}{du^k}(f(G_2(u), u))|_{u=0^-} = 0$ for $0 \leq k \leq n_2 - 1$, $\frac{d^{n_2}}{du^{n_2}}(f(G_2 u), u))|_{u=0^-} \neq 0$. After this observation, we can use the same argument as in the proof of (i) of Theorem 3.2 in [12] to complete the proof. Recall that this proof requires that w is an odd function and this assumption is satisfied by the function (2.5). Note that the final estimate will produce the decay rate of $O(a^{n_1+\frac{9}{4}})$ for the right-side of the corner point and the decay rate of $O(a^{n_2+\frac{9}{4}})$ for the left-side of the corner point. Therefore, we conclude that the decay rate at the corner point is $O(a^{n_2+\frac{9}{4}})$ where is $n = \min\{n_1, n_2\}$.

Proof of (ii): By assumption, the left and right normal directions at the corner point $p = (0,0)$ are different. Without loss of generality, we may assume that $s_0 = 0$. It follows that $s_0 = 0$ does not correspond to the left normal direction $\vec{n}(p^-)$. Therefore, by part (i) of the theorem, on the left section of the boundary curve $\{(G_2(u), u) : -\epsilon < u < 0\}$, the shearlet transform has asymptotic decay rate as fast or faster than $a^{n_2+\frac{9}{4}}$ as $a \to 0^+$.

We first consider the case $n_2 + \frac{9}{4} > \frac{n_1}{2} + \frac{3}{4}$. In this case, (ii) will be proved if we can show that the estimate of the shearlet transform on the right-section of the boundary curve $\{(G_1(u), u) : 0 \le u < \epsilon\}$ yields the exact decay rate $a^{\frac{n_1}{2}+\frac{3}{4}}$ as $a \to 0^+$. Since $s_0 = 0$ (and hence $\theta_0 = 0$), we must have $G_1'(0^+) = 0$ and, thus, we have that $G_1(u) = Au^2 + O(u^3)$ for $u \in [0, \epsilon)$.

Following the proof of part (iii) of Theorem 3.1, we examine the integral I_1, given by (4.2), using the shearlet generator ψ, at $s_0 = 0, p = (0,0), l = 0$. By splitting the integral $I_1(a, 0, 0, 0)$ into $I_{11}(a, 0, 0, 0) + I_{12}(a, 0, 0, 0)$ as in (5.2), we find that

$$\begin{aligned} & \lim_{a\to 0^+} a^{-(\frac{n_1}{2}+\frac{3}{4})} (2\pi i)^{n_1} I_{11}(a, 0, 0, 0) \\ = \quad & (2\pi i)^{n_1} \int_0^\infty \int_0^\infty \int_{-1}^1 e^{-2\pi i \rho (Ay^2 + ty)} y^{n_1} w(\rho)\, v(t)\, dt\, d\rho\, dy \\ := \quad & T_{n_1}(A). \end{aligned}$$

Note that, unlike the similar expression in the proof of Theorem 3.1, the integral in y ranges over $[0, \infty)$ rather than $(-\infty, \infty)$ due to the fact that we are examining the integral on the right section of the boundary curve near $p = (0, 0)$. As in the proof of part (iii) of Theorem 3.1, to estimate of $T_{n_1}(A)$ we need to consider two separate cases for $A = 0$ and $A \neq 0$.

For $A = 0$, we observe that

$$\begin{aligned} T_{n_1}(0) &= (2\pi i)^{n_1} \int_0^\infty \int_0^\infty \int_{-1}^1 e^{2\pi i \rho t y} y^{n_1} w(\rho)\, v(t)\, dt\, d\rho\, dy \\ &= (2\pi i)^{n_1} \int_0^\infty \int_0^\infty \check{v}(\rho y)\, y^{n_1} w(\rho)\, dy\, d\rho. \end{aligned}$$

In order to show that $\mathrm{Real}(T_{n_1}(0)) \neq 0$ or $T_{n_1}(0) + \overline{T_{n_1}(0)} \neq 0$, we separate the discussion into the two cases where n_1 is even and n_1 is odd.

If n_1 is even, we have

$$\begin{aligned} & T_{n_1}(0)+\overline{T_{n_1}(0)} \\ = \; & (2\pi i)^{n_1} \int_0^\infty \int_0^\infty \int_{-1}^1 \left(e^{2\pi i\rho t y}+e^{-2\pi i \rho t y}\right) y^{n_1} w(\rho)\, v(t)\, dt\, d\rho\, dy \\ = \; & (2\pi i)^{n_1} \int_0^\infty \int_0^\infty (\check{v}(\rho y)+\check{v}(-\rho y))\, y^{n_1} w(\rho)\, dy\, d\rho \\ = \; & (2\pi i)^{n_1} \int_{-\infty}^\infty \check{v}(y)\, y^{n_1}\, dy \int_0^\infty w(\rho)\, \rho^{-(n_1+1)} d\rho \\ = \; & v^{(n_1)}(0) \int_0^1 w(\rho)\, \rho^{-(n_1+1)} d\rho > 0. \end{aligned}$$

If n_1 is odd, a similar calculation shows that

$$\begin{aligned} & T_{n_1}(0)+\overline{T_{n_1}(0)} \\ = \; & (2\pi i)^{n_1} \int_0^\infty \int_0^\infty \int_{-1}^1 \left(e^{2\pi i\rho t y}-e^{-2\pi i \rho t y}\right) y^{n_1} w(\rho)\, v(t)\, dt\, d\rho\, dy \\ = \; & (2\pi i)^{n_1} \int_0^\infty \int_0^\infty (\check{v}(\rho y)-\check{v}(-\rho y))\, y^{n_1} w(\rho)\, dy\, d\rho \\ = \; & (2\pi i)^{n_1} \int_{-\infty}^\infty \check{v}(y)\, y^{n_1}\, dy \int_0^\infty w(\rho)\, \rho^{-(n_1+1)} d\rho \\ = \; & v^{(n_1)}(0) \int_0^1 w(\rho)\, \rho^{-(n_1+1)} d\rho > 0. \end{aligned}$$

Then, as in the proof of part (iii) of Theorem 3.1, we can estimate for $T'_{n_1}(A)$ and conclude that, for $|A| \le \frac{1}{M}$, we have $\text{Real}(T_{n_1}(A)) \ge \frac{1}{2} T_{n_1}(0) \ne 0$, for $n_1 = 0, \dots, N_0$.

For $|A| \ge \frac{1}{M}$, we need to consider the second shearlet transform defined using the shearlet generator ψ_M. Then, a direct calculation gives that

$$\begin{aligned} T_{n_1}(A) \; = \; & \tfrac{1}{2\sqrt{A}} \int_{-1}^1 \int_0^{\frac{1}{M^2}} e^{\pi i \rho \frac{1}{2A} t^2} \rho^{-(n_1+\frac{1}{2})} e^{-(\frac{1}{M^2\rho}+\frac{1}{1-M^2\rho})}\, v^{(n_1)}(t) \\ & \times \left(\tfrac{1-i}{2} + \int_{\sqrt{\frac{\rho}{A}}t}^0 e^{-\frac{\pi}{2} i y^2} dy \right) d\rho\, dt \\ = \; & \tfrac{M^{2n_1+1}}{2\sqrt{A}} \int_{-1}^1 \int_0^1 e^{\pi i \rho \frac{1}{2AM^2} t^2} \rho^{-(n_1+\frac{1}{2})} e^{-(\frac{1}{\rho}+\frac{1}{1-\rho})}\, v^{(n_1)}(t) \\ & \times \left(\tfrac{1-i}{2} + \int_{\sqrt{\frac{\rho}{AM^2}}t}^0 e^{-\frac{\pi}{2} i y^2} dy \right) d\rho\, dt. \end{aligned}$$

Since $|t| \le 1$, $0 \le \rho \le 1$ and $AM \ge 1$, it is easy to see that $|\int_{\sqrt{\frac{\rho}{AM^2}}t}^0 e^{-\frac{\pi}{2} i y^2} dy| \le M^{-\frac{1}{2}} \le \frac{1}{4}$, which is dominated by $\frac{1-i}{2}$ since $M \ge 16$. The rest of the proof is then the same as the proof of part (iii) of Theorem 3.1.

This completes the proof of part (ii) of Theorem 3.2 for the case $n_2 + \frac{9}{4} > \frac{n_1}{2} + \frac{3}{4}$.

We next consider the case $n_2 + \frac{9}{4} \leq \frac{n_1}{2} + \frac{3}{4}$. The estimate of this case follows from part (i) of the theorem and the observation we made at the beginning of part of (ii) this proof. Note that, for this argument, we can use the shearlet transform with shearlet generator ψ or ψ_M, without any difference in the conclusion.

This completes the proof of part (ii) of Theorem 3.2.

6. Conclusion

We have shown that the continuous shearlet transform provides a precise geometric characterization of the set of discontinuities of piecewise smooth functions of the form

$$h = \sum_{i=1}^{N} f_i \, \chi_{S_i}, \tag{6.1}$$

where, for each i, f_i is a C^∞ smooth function with values in $\mathbb{R}^2$ and the compact regions $S_i \subset \mathbb{R}^2$ are disjoint, with piecewise smooth boundary.

The arguments presented in this paper can be extended to the more general situation where the regions S_i in (6.1) are not disjoint, but share a common boundary. To deal with the case, let us consider regions S_1 and S_2 having a common boundary curve γ and denote by f_1 and f_2 the smooth functions on S_1 and S_2 respectively. To analyze $\mathcal{SH}_\psi B(a,s,p)$, where $B = \chi_h$, for a point $p \in \gamma$, we can follow the strategy we applied to deal with corner points that consists in examining the asymptotic decay rate (as $a \to 0$) from the right and from the left neighbourhood of p. Using this idea, from the results proved above in this paper, we can derive an asymptotic decay rate for $f_1(x)\,\chi_{S_1}(x)$ when $x \to p \in \gamma$ and another asymptotic decay rate for $f_2(x)\,\chi_{S_2}(x)$ when $x \to p \in \gamma$. The asymptotic decay rate of $\mathcal{SH}_\psi B(a,s,p)$, as $a \to 0$, will then be obtained as the minimum of the two decay rates.

The results presented in this paper can be generalized to the situation where the functions f_i are not C^∞ but only C^K for some $K \in \mathbb{N}$. Under this modified assumption, when $p \notin \partial S$ or $p \in \partial S$ and s does not correspond to the normal direction (cases (i-ii) of Theorem 3.1), we cannot conclude that $\mathcal{SH}_\psi B(a,s,p)$ decay faster than a^N, as $a \to 0$, for all $N \in \mathbb{N}$. However, if K is sufficiently large, we can derive that $\mathcal{SH}_\psi B(a,s,p)$ decay faster than a^N, as $a \to 0$, for all $N \leq N_0(K)$, where $N_0(K)$ increases with K. For $p \in \partial S$ and s corresponding to the normal direction (cases (iii) of Theorem 3.1), we can derive the same estimate of Theorem 3.1 provided that $K \geq 4$.

In conclusion, our result shows that the continuous shearlet transform identifies both the location and orientation of the boundary curves ∂S_i, including the corner points. This is a major extension of the prior result that was valid only in the case of piecewise constant functions. This new powerful result sets the theoretical groundwork for the application of the shearlet framework to a wider class of problems from image processing.

Finally, we remark that multiscale methods for the analysis and detection of singularities have a long history of applications to image processing problems. Among the classical results, we recall the algorithms for edge detection and analysis of singularities by Mallat, Hwang and Zhong [26, 27]. This work stimulated many generalizations and applications in areas including medical and seismic imaging (cf. [16, 20]). In more recent years, several improved algorithms were introduced incorporating the ideas of directional multiscale analysis. In particular, a very competitive shearlet-based algorithm for edge analysis and detection was introduced by the authors and their collaborators in [29, 31]; some applications of these ideas to problems of feature extraction and classification can be found in [6, 24, 30, 32].

Acknowledgments. The authors acknowledge support from NSF grant DMS 1008900//1008907; the second author also acknowledges support from NSF grants DMS 1005799, 1320910.

References

[1] J. Bros and D. Iagolnitzer, *Support essentiel et structure analytique des distributions*, Seminaire Goulaouic-Lions-Schwartz, 19, 1975-76.

[2] E. J. Candès and D. L. Donoho, *Continuous curvelet transform: I. Resolution of the wavefront set*, Appl. Comput. Harmon. Anal., 19 (2005), pp. 162–197.

[3] A. Córdoba and C. Fefferman, *Wave packets and fourier integral operators*, Communications in Partial Differential Equations, 3(11) (1978), pp. 979–1005.

[4] S. Dahlke, G. Steidl, and G. Teschke, *The Continuous Shearlet Transform in Arbitrary Space Dimensions*, J. Fourier Anal. Appl., 16(3) (2009), pp. 340–364.

[5] S. Dahlke, and G. Teschke, *The Continuous Shearlet Transform in Arbitrary Space Dimensions: Variations of a Theme* in: *Group Theory: Classes, Representations and Connections, and Applications*, (C.W. Danellis, Ed.), Nova Science Publishers, 2010, pp. 167–175.

[6] M.A. Duval-Poo, F. Odone, and E. De Vito, *Edges and corners with shearlets*, to appear in IEEE Trans. Image Process. 2015

[7] G. Easley, D. Labate, and W.-Q Lim, *, Sparse directional image representations using the discrete shearlet transform*, Appl. Comput. Harmon. Anal. 25 (2008), pp. 25–46.

[8] P. Gérard, *Moyennisation et regularitè deux-microlocale*, Ann. Scient. Ec. Norm. Sup., 4eme serie, 23 (1990), pp. 89–121.

[9] P. Grohs, *Continuous shearlet frames and resolution of the wavefront set*, Monatshefte för Mathematik, 164(4) (2011), pp. 393–426.

[10] A. Grossmann, *Wavelet transforms and edge detection*. In *Stochastic Processes in Physics and Engineering* (S. Albeverio, P. Blanchard, M. Hazewinkel, and L. Streit, Eds.), volume 42 of Mathematics and Its Applications, Springer Netherlands, 1988, pp. 149–157.

[11] K. Guo, R. Houska, and D. Labate, *Microlocal analysis of singularities from directional multiscale representations*, Proceedings from: Approximation Theory XIV: San Antonio 2013 (April 7-10, 2013, San Antonio, Texas). Springer Proceedings in Mathematics & Statistics, 83, 2014, pp. 173-196 .

[12] K. Guo, and D. Labate, *Characterization and analysis of edges using the continuous shearlet transform*, SIAM on Imaging Sciences, 2 (2009), pp. 959–986.

[13] K. Guo, and D. Labate, *Analysis and detection of surface discontinuities using the 3D continuous shearlet transform*, Appl. Comput. Harmon. Anal., 30 (2011), pp. 231–242.

[14] K. Guo, and D. Labate, *Characterization of piecewise-smooth surfaces using the 3D continuous shearlet transform*, J. Fourier Anal. Appl., 18 (2012), pp. 488–516.

[15] K. Guo, D. Labate and W. Lim, *Edge analysis and identification using the continuous shearlet transform*, Appl. Comput. Harmon. Anal., 27(1) (2009), pp. 24–46.

[16] F. J. Herrmann, *Singularity characterization by monoscale analysis*, Appl. Comput. Harmon. Anal., 11(4) (2001), pp. 64–88.

[17] M. Holschneider, *Wavelets. Analysis tool*, Oxford University Press, Oxford, 1995.

[18] S. Jaffard, *Pointwise smoothness, two-microlocalization and wavelet coefficients*, Publications Matematiques, 35 (1991), pp. 155–168.

[19] S. Jaffard, Y. Meyer, *Wavelet methods for pointwise regularity and local oscillations of functions*, Memoirs of the AMS, 123 n.587 (1996).

[20] J. H. Kaspersen, T. Lango, F. Lindseth, *Wavelet-based edge detection in ultrasound images*, Ultrasound Med Biol, 27 (2001), pp. 89–99.

[21] G. Kutyniok and D. Labate, *Resolution of the Wavefront Set using Continuous Shearlets*, Trans. Amer. Math. Soc., 361 (2009), pp. 2719–2754.

[22] G. Kutyniok, P. Petersen, *Classification of Edges using Compactly Supported Shearlets*, preprint, arXiv:1411.5657

[23] G. Kutyniok, M. Shahram, and X. Zhuang, *ShearLab: A Rational Design of a Digital Parabolic Scaling Algorithm*, SIAM J. Imaging Sci., 5(4) (2012), pp. 1291–1332.

[24] D. Labate, F. Laezza, B. Ozcan, P. Negi, M. Papadakis, *Efficient processing of fluorescence images using directional multiscale representations*, Math. Model. Nat. Phenom., 9(5) (2014), pp. 177–193.

[25] D. G. Lowe, *Distinctive Image Features from Scale-Invariant Keypoints*, Int. J. Comp. Vision 60 (2004), pp. 91–110.

[26] S. Mallat and W. L. Hwang, *Singularity detection and processing with wavelets*, IEEE Trans. Inf. Theory, 38(2) (1992), pp. 617–643.

[27] S. Mallat and S. Zhong, *Characterization of signals from multiscale edges*, IEEE Trans. Pattern Anal. Mach. Intell., 14(7) (1992), pp. 710–732.

[28] Y. Meyer, *Wavelets and Operators*, Cambridge Stud. Adv. Math. vol. 37, Cambridge Univ. Press, Cambridge, UK, 1992.

[29] D. P. O'Leary, D. A. Schug, G. R. Easley, *Three-dimensional shearlet edge analysis*, Proc. SPIE 8058, Independent Component Analyses, Wavelets, Neural Networks, Biosystems, and Nanoengineering IX, 2011.

[30] B. Ozcan, P. Negi, F. Laezza, M. Papadakis, and D. Labate, *Automated detection of soma location and morphology in neuronal network cultures*, PLos ONE, 10(4), (2015).

[31] S. Yi, D. Labate, G. R. Easley, and H. Krim, *A Shearlet Approach to Edge Analysis and Detection*, IEEE Trans. Image Process., 18 (2009), pp. 929–941.

[32] S. Zhou, J. Shi, J. Zhu, Y. Cai, R. Wang, *Shearlet-based texture feature extraction for classification of breast tumor in ultrasound image*, Biomedical Signal Processing and Control, 8(6) (2013), pp. 688.

[33] D. Ziou, and S. Tabbone, *Edge Detection Techniques An Overview*, International Journal of Pattern Recognition and Image Analysis, 8(4) (1998), pp. 537–559.